International Journal of Bifurcation and Chaos, Vol. 7, No. 7 (1997) 1555–1577

BASIN FRACTALIZATION DUE TO FOCAL POINTS IN A CLASS OF TRIANGULAR MAPS

GIAN-ITALO BISCHI
Istituto di Scienze Economiche, Università di Urbino, I-61029 URBINO (Italy)

LAURA GARDINI
Dipartimento di Metodi Quantitativi, Università di Brescia, I-25122 BRESCIA (Italy)
and *Istituto di Scienze Economiche, Università di Urbino, I-61029 URBINO (Italy)*

Received October 1, 1996; Revised January 7, 1997

For a class of rational triangular maps of a plane, characterized by the presence of points in which a component assumes the form $\frac{0}{0}$, a new type of bifurcation is evidenced which creates loops in the boundaries of the basins of attraction. In order to explain such bifurcation mechanism, new concepts of *focal point* and *line of focal values* are defined, and their effects on the geometric behavior of the map and of its inverses are studied in detail. We prove that the creation of loops, which generally constitute the boundaries of lobes of the basins issuing from the focal points, is determined by contacts between basin boundaries and the line of focal values. A particular map is proposed for which the sequence of such contact bifurcations occurs, causing a fractalization of basin boundaries. Through the analytical and the numerical study of this example new structures of the basins of attraction are evidenced, characterized by fans of stable sets issuing from the focal points, assuming the shape of lobes and arcs, the latter created by the merging of lobes due to contacts between the basin boundaries and the critical curve LC.

1. Introduction

In this work we present a new kind of bifurcation, which causes the fractalization of the basin boundaries in a class of triangular maps arising in applicative contexts [Bischi & Naimzada, 1995; Bischi & Gardini, 1996]. Such class of maps, deduced in [Bischi & Gardini, 1996], has the triangular structure $x' = \Phi(x, y)$; $y' = \Psi(y)$, defined by

$$T: \begin{cases} x' = \dfrac{\rho xy + f(x)}{1 + \rho y} \\ y' = \quad 1 + \rho y \end{cases} \tag{1}$$

where $\rho \in (0, 1)$ is a parameter and $f : \mathbb{R} \to \mathbb{R}$ is a function of class $\mathcal{C}^2$.

It is known that the asymptotic behavior of a triangular map is related to the dynamics of a one-dimensional map [Gardini & Mira, 1993], and this is particularly simple in the class (1). But the determination of the basins of attraction requires a global study of (1) in its two-dimensional phase space, and in particular of its critical sets LC_{-1} and LC that, following the notation introduced in [Gumowski & Mira, 1980], represent the sets of critical points and of critical values respectively.

The peculiarity of the class of triangular maps (1) is given by the fact that T is not defined in the whole plane $\mathbb{R}^2$, due to the presence, in the first component $\Phi(x, y)$, of the denominator which vanishes along the line δ_s of equation $y = -\frac{1}{\rho}$

(*singular line*). In particular, the existence, on the singular line, of points in which the function $\Phi(x, y)$ assumes the form $\frac{0}{0}$ plays a special role in the characterization of the basins of attraction, and can give rise to sequences of bifurcations causing a fractalization of basin boundaries. These particular points will be called *focal points* following the terminology introduced by Mira in his pioneering work [Mira, 1981].[1]

The basin bifurcations studied in the present paper are not the result of a contact between basin boundaries and critical curves (as often occurs in noninvertible maps defined on the whole plane, see [Mira *et al.*, 1996]) and are only possible if focal points are present.

Such basin bifurcations can also be seen in different kinds of noninvertible maps with vanishing denominator, like those considered in [Bischi & Gardini, 1995; Billings & Curry, 1996; Bischi & Naimzada, 1996]. However, to our knowledge, this is the first study describing the bifurcation mechanism related to the presence of focal points.

Roughly speaking, these bifurcations may be characterized by the creation of loops in basin boundaries, issuing from the *focal points*, due to the contacts of basin boundaries with the set of *focal values*.

The plan of the work is as follows. In Sec. 2 some general features of the class of maps (1) are given, concerning ω-limit sets and basin boundaries, together with the definitions, and the main properties, of the focal points and the set of focal values. In particular, in Secs. 2.1 and 2.2 the spectral properties and the asymptotic behavior of (1) are analyzed. In Secs. 2.3 and 2.4 the main results are given, concerning the properties of focal points. Here a one-to-one correspondence between the slopes of curves issuing from a focal point and the position of the images along the line of focal values is given, which is the basis to explain the geometric action of T, often counterintuitive, near the focal points and near the focal values. The mechanism which creates "loops" issuing from focal points, which generally constitute the boundaries of "lobes" of attraction basins, is explained in detail. The "fan" of stable sets issuing from the focal points and the fractalization mechanism are explained in Sec. 2.4 on the basis of the propositions of Sec. 2.3. In Sec. 2.5 some properties of the critical sets LC_{-1} and LC of the maps (1) are given, and in Sec. 2.6 a peculiar property of the inverses of T is proved, which may be considered an analytical proof for the geometric behavior of T^{-1}.

In Sec. 3 a particular example, with the function f given by a cubic polynomial, is considered, with particular emphasis on the structure of the basins and their bifurcations. The parameters' values at which the bifurcations creating lobes of the basins occur are analytically determined, and the particular structure of the boundaries separating the basins of different coexisting attractors are analyzed through numerical exploration, guided by the results of Sec. 2.

2. General Properties of the Triangular Maps T

2.1. *Domain and range of the map T*

The maps T of the form (1) are not defined in the whole plane because the denominator of the first component $\Phi(x, y)$ vanishes in the points of the line δ_s of equation $y = -\frac{1}{\rho}$ (*singular line*). Thus, in order to have a well defined two-dimensional recurrence, we must exclude from the phase plane of T the singular line as well as all its preimages of any rank. These preimages belong to a sequence of lines located below the singular line, i.e. in the half plane with $y < -\frac{1}{\rho}$. In fact the second component $\Psi(y)$ of T can be easily inverted to obtain

$$y = \frac{y' - 1}{\rho} \tag{2}$$

from which we deduce that the points which are mapped by T in the singular line are the points of the line δ_s^{-1} of equation $y = -\frac{1+\rho}{\rho^2}$, which is below δ_s, and the points which are mapped in the singular line after n iterations of T are located on the line δ_s^{-n} of equation

$$y = -\frac{\sum_{k=0}^{n} \rho^k}{\rho^{n+1}} = -\frac{1 - \rho^{n+1}}{\rho^{n+1} - \rho^{n+2}}. \tag{3}$$

All these lines are below δ_s, as $\delta_s^{-(n+1)}$ is below δ_s^{-n} for each $n \geq 1$. Thus the phase space of the recurrence defined by the map T is given by

$$A = \mathbb{R}^2 \Big\backslash \bigcup_{n=0}^{\infty} \delta_s^{-n} \tag{4}$$

[1] In our definition of focal point, given in Sec. 2, we require not only that the map assumes the form $\frac{0}{0}$ but also the existence of finite limit values. The set of such values will be denoted as the locus of *focal values*.

where δ_s^{-n} are defined by (3). Clearly T maps A into itself but not onto. In fact the range of T cannot include the x-axis because $y' = 0$ is got by (1) only if $y = -\frac{1}{\rho}$, and such a value of y does not belong to the domain of T.

2.2. *Spectral properties and asymptotic behavior of T*

The maps T are defined in every point of the half-plane $y > -\frac{1}{\rho}$. Furthermore any trajectory starting in the set A enters such a half plane. This is due to the simple form of the second component $\Psi(y)$ of the map T, whose iteration gives the sequence

$$y_n = \sum_{k=0}^{n-1} \rho^k + \rho^n y_0 = \frac{1-\rho^n}{1-\rho} + \rho^n y_0 \,. \qquad (5)$$

For $\rho \in (0, 1)$ such sequence is monotonically convergent to

$$y^* = \frac{1}{1-\rho}, \qquad (6)$$

increasing if $y_0 < y^*$, decreasing if $y_0 > y^*$. This implies that the line $y = y^*$, which is mapped into itself by T, is globally attracting for the trajectories of T. In other words, the limit set of any trajectory of the map T belongs to the trapping line $y = y^*$ (*line of ω-limit sets*) and is an invariant set of the restriction of T to such line, which can be identified with the one-dimensional map (*limiting map*)

$$x' = h_\rho(x), \quad h_\rho(x) = \rho x + (1-\rho) f(x) \,. \qquad (7)$$

It is easy to see that the limiting map $h_\rho(x)$ has the same fixed points as the map $f(x)$, but this property no longer holds for cycles of higher period, that is, for k-cycles with $k > 1$.

Any k-cycle of the two-dimensional map T, which necessarily belongs to the line of ω-limit sets, has the property that its projection on the x-axis is a k-cycle of the one-dimensional map given in (7). It is also immediate to see that the stability properties of the cycles of T, and all the local bifurcations involving attracting sets of T, can be deduced from the properties of $h_\rho(x)$. These are consequences of the spectral properties of T, whose Jacobian matrix is the triangular matrix

$$DT(x, y) = \begin{bmatrix} J_{11} & J_{12} \\ 0 & \rho \end{bmatrix} \qquad (8)$$

where $J_{11} = \frac{\rho y + f'(x)}{1+\rho y}$ and $J_{12} = \frac{\rho(x - f(x))}{(1+\rho y)^2}$. On the line of the ω-limit sets DT becomes

$$DT(x, y^*) = \begin{bmatrix} h'_\rho(x) & \rho(1-\rho)(x - f(x)) \\ 0 & \rho \end{bmatrix} \qquad (9)$$

where $h'_\rho(x)$ is the derivative of the limiting function (7). $DT(x, y^*)$ becomes diagonal at any fixed point (x^*, y^*), with eigenvalues

$$\lambda_1 = h'_\rho(x^*) = \rho + (1-\rho) f'(x) \quad \text{and} \quad \lambda_2 = \rho \,. \qquad (10)$$

The eigenvalue λ_1 coincides with the multiplier of the fixed point x^* of the one-dimensional limiting map (7), and λ_2 always satisfies the constraints for the stability, since $0 < \rho < 1$. Moreover, being $DT(x^*, y^*)$ a diagonal matrix, we have that the invariant set issuing from the fixed point and related to λ_1 is the line $y = y^*$, whereas the local stable manifold issuing from the fixed point and related to λ_2 is the line $x = x^*$. Similarly, a set $\mathcal{C}_k = \{(x_1, y^*), \ldots, (x_k, y^*)\}$ is a k-cycle of T, with $k > 1$, if and only if $\{x_1, \ldots, x_k\}$ is a k-cycle of $h_\rho(x)$, and the Jacobian matrix of T^k, given by $DT^k = \prod_{i=1}^k DT(x_i, y^*)$, is upper triangular with eigenvalues

$$s_1 = \prod_{i=1}^{k} h'_\rho(x_i) \quad \text{and} \quad s_2 = \rho^k \,. \qquad (11)$$

The eigenvalue s_1 coincides with the multiplier of the k-cycle $\{x_1, \ldots, x_k\}$ of the map $h_\rho(x)$, and the related eigendirection is along the line $y = y^*$, whereas the eigendirection related to s_2 is transverse to that line. Hence any cycle $\mathcal{C}_k$ of T possesses a local stable set W^s_{loc} transverse to the line of the ω-limit sets. If the corresponding cycle $\{x_1, \ldots, x_k\}$ is attracting for the limiting map $h_\rho(x)$ then $\mathcal{C}_k$ is an attracting node for the map T, whereas if $\{x_1, \ldots, x_k\}$ is repelling for h_ρ then $\mathcal{C}_k$ is a saddle for T (note that a cycle of T cannot be a focus because the eigenvalues (11) are real, and cannot be a repelling node because $0 < s_2 < 1$). Thus in any case we have a local stable set transverse to the line of ω-limit sets.

From the arguments outlined above the dynamics of the triangular maps (1) appear to be rather simple since the ω-limit sets of T only depend on the one-dimensional limiting map (7). For each initial condition in the domain A, defined in (4), the trajectory approaches the line of the ω-limit sets $y = y^*$ and may be either divergent (i.e. convergent

to an attractor at infinite distance on that line, say $(\pm\infty, y^*)$, represented by a point of the Poincaré Equator), or bounded (i.e. convergent to some absorbing interval or cyclic intervals on that line).

However the analysis is not so simple if we want to determine the basins of the different coexisting attractors, such as D_∞, defined as the set of points of A generating unbounded trajectories of T, or, equivalently, the complementary set $A\backslash D_\infty$, which is the set of points having bounded trajectories. Also the points of this set (which may be the whole phase plane A if $D_\infty = \emptyset$) may belong to the different basins of coexisting bounded (or at finite distance) attracting sets. The determination of the basins is very important also in applications, and the study of the limiting map $h_\rho(x)$ gives no help in this direction. It is necessary to consider the global two-dimensional properties of T, and its critical curves when T is noninvertible.

In general the boundaries of a basin are obtained by taking the stable sets of some cycles on it. In the case of maps (1) such cycles can only be of saddle type, and located on the line of ω-limit sets. To get the stable set W^s of a saddle it is enough to take the preimages of any rank of a local stable set W^s_{loc}, that is $W^s = \bigcup_{n=0}^{\infty} T^{-n}(W^s_{loc})$. As explained above W^s_{loc} is transverse to the line $y = y^*$ and its preimages cannot have other cycles at finite distance as limit sets, since all the cycles of T belong to the line $y = y^*$. Thus, due to the expansive character of $\Psi^{-1}(y)$, defined in (2), such preimages must necessarily reach, in a finite number of steps, the line $y = 0$, which does not belong to the range of T. However we shall see that all these preimages must necessarily cross the singular line $y = -\frac{1}{\rho}$ through points in which the first component $\Phi(x, y)$ assumes the form $\frac{0}{0}$.

2.3. *Focal points and focal values: Definitions and properties*

Definition 1. A *focal point* of a map $T(x, y)$ is a point (x_F, y_F) in which at least a component of T assumes the form $\frac{0}{0}$ and for smooth simple arcs transverse to the singular line, with parametric representation $\gamma(t)$ such that $\gamma(0) = (x_F, y_F)$, $\lim_{t\to 0} T(\gamma(t))$ is finite. The set of all such finite values, obtained with different curves γ, constitutes the set of *focal values*.

Of course, for the class of triangular maps (1) this can only occur for the first component $\Phi(x, y)$ and, since the denominator only vanishes in the points of the singular line $y = -\frac{1}{\rho}$, all the focal points of T must necessarily belong to this line. On this line the numerator of $\Phi(x, y)$ becomes $f(x) - x$, hence it vanishes if and only if x satisfies $f(x) = x$, i.e. at every fixed point of the function $f(x)$ [and thus also of the limiting map (7)]. It follows that the limit of $\Phi(x, y)$ as $(x, y) \to (x_0, -\frac{1}{\rho})$, where x_0 is not a fixed point of $f(x)$, is either $(+\infty, 0)$ or $(-\infty, 0)$, and a focal point is necessarily of type $(x^*, -\frac{1}{\rho})$, where x^* is a fixed point of $f(x)$. However, according to the definition given above, we have also to see whether the function $\Phi(x, y)$ takes finite limit values as $(x, y) \to (x^*, -\frac{1}{\rho})$. For this purpose let us consider a smooth simple arc γ, transverse to the singular line, represented by the parametric equations

$$\gamma(t): \begin{cases} x = \varphi(t) = x^* + t\varphi_0 + t^2\varphi_1 + O(t) \\ y = \psi(t) = -\frac{1}{\rho} + t\psi_0 + t^2\psi_1 + \overline{O}(t), \\ \qquad\qquad \text{with} \quad \psi_0 \neq 0 \end{cases} \tag{12}$$

with $O(t)$ and $\overline{O}(t)$ representing higher order terms. We get

$$\lim_{t\to 0} T(\gamma(t)) = \left(x^* + \frac{\varphi_0}{\rho\psi_0}(f'(x^*) - 1), 0\right).$$

Let $m = \frac{\psi_0}{\varphi_0}$ be the slope of the tangent to the smooth arc γ in the point $(x^*, -\frac{1}{\rho})$, assuming $m \to \infty$ when $\varphi_0 = 0$. Then we have

$$\lim_{t\to 0} T(\gamma(t)) = (u_m, 0), \tag{13}$$

$$\text{with} \qquad u_m = x^* + \frac{f'(x^*) - 1}{\rho m}.$$

It is clear that on varying m in $\mathbb{R}\backslash\{0\}$ all the points of the line $y = 0$ are obtained, provided that x^* is a fixed point for which $f'(x^*) \neq 1$. Thus the line δ_0, of equation $y = 0$, represents the set of focal values for the maps (1). A situation in which $f'(x^*) = 1$ can be considered as a bifurcation case, which may change the number of fixed points of $f(x)$, and thus of the focal points of T. Considering a generic case we shall assume the following:

Assumption (H). We assume that any fixed point x^* of $f(x)$ satisfies $f'(x^*) \neq 1$.

We can now give the following:

Proposition 1. *Any point* $F_k = (x_k^*, -\frac{1}{\rho})$, *where* x_k^* *is a fixed point of* $f(x)$ *satisfying Assumption* (H), *is a focal point of the class of maps* (1). *For each focal point the set of focal values is the line* δ_0 *of equation* $y = 0$.

From the computation of (13) it is clear that if we consider an arc γ deprived of the point on the singular line, say $\gamma = \gamma_- \cup \gamma_+$ where γ_- and γ_+ denote the portions below and above the singular line respectively, and such that the closure $\overline{\gamma}$ is a smooth curve through a focal point, then $T(\gamma)$ is a bounded arc, $T(\gamma) = T(\gamma_-) \cup T(\gamma_+)$, with $T(\gamma_-)$ and $T(\gamma_+)$ below and above the line of focal values respectively, and such that the closure $\overline{T(\gamma)}$ is smooth in the point $(u_m, 0)$ of the focal line, u_m depending on the slope m of $\overline{\gamma}$ in the focal point according to (13) (see the schematic picture in Fig. 1(a). It is worth noticing that different arcs γ_α, such that $\overline{\gamma_\alpha}$ have all the same tangent of slope m in the focal point, are mapped into arcs $T(\gamma_\alpha)$ such that $\overline{T(\gamma_\alpha)}$ all cross the line of focal values at the same point $(u_m, 0)$ but with different slopes, as schematically shown in Fig. 1(b). This property can be proved by direct computation. In fact, considering an arc γ parameterized as in (12), we have that the tangent to the arc $\overline{T(\gamma_\alpha)}$ in $(u_m, 0)$ has slope S given by

$$S = \frac{\rho^2 \psi_0^3}{\rho \varphi_0 \psi_0^2 + \psi_0 \left[\frac{\varphi_0^2}{2} f''(x^*) - \varphi_1 + f'(x^*)\varphi_1 \right] + \varphi_0 \psi_1 [1 - f'(x^*)]}.$$

Assuming φ_0 and ψ_0 fixed and varying φ_1 and ψ_1 in order to get a family of arcs γ_α all tangent to the same line, we see that the slope S takes different values.

A different situation is obtained if we consider the image by T of an arc $\gamma = \gamma_- \cup \gamma_+$ as above, but such that the closure $\overline{\gamma}$ intersects the singular line in a point $(x_0, -\frac{1}{\rho})$ which is not a focal point. By using the parametric representation

$$\overline{\gamma(t)} : \begin{cases} x = \varphi(t) = x_0 + t\varphi_0 + O(t) \\ y = \psi(t) = -\frac{1}{\rho} + t\psi_0 + \overline{O}(t), \quad \psi_0 \neq 0 \end{cases} \tag{14}$$

we get $\lim_{t \to 0 (\text{on } \gamma_\pm)} T(\gamma(t)) = (\frac{-x_0 + f(x_0)}{0_\pm}, 0) = (\pm\infty, 0)$ or $(\mp\infty, 0)$ according to $(f(x_0) - x_0) > 0$ or $(f(x_0) - x_0) < 0$ respectively. In any case $T(\gamma_-)$ and $T(\gamma_+)$ are two disjoint unbounded arcs, $T(\gamma_-(t))$ below and $T(\gamma_+(t))$ above the line of focal values, as qualitatively shown in Figs. 1(c) and 1(d). These results are summarized by the following propositions:

Proposition 2. *Any smooth simple arc* $\gamma = \gamma_- \cup \gamma_+$, *where* γ_- *and* γ_+ *denote the components below and above the singular line respectively, such that the closure* $\overline{\gamma}$ *has a tangent of slope* $m \neq 0$ *in the focal point* $F = (x^*, -\frac{1}{\rho})$, *is mapped by* T *into a bounded arc,* $T(\gamma) = T(\gamma_-) \cup T(\gamma_+)$, *with* $T(\gamma_-)$ *and* $T(\gamma_+)$ *below and above the line of focal values respectively, and such that the closure* $\overline{T(\gamma)}$ *is a smooth curve through the point* $(u_m(x^*), 0)$ *of the focal line with*

$$u_m(x^*) = x^* + \frac{f'(x^*) - 1}{\rho m}. \tag{15}$$

Different arcs γ_α *such that* $\overline{\gamma_\alpha}$ *have all the same tangent in the focal point* F *with slope* $m \neq 0$ *are mapped into different arcs* $T(\gamma_\alpha)$ *such that each* $\overline{T(\gamma_\alpha)}$ *crosses the line of focal values in the point* $(u_m(x^*), 0)$ *with slopes generally different.*

Proposition 3. *Any smooth simple arc* $\gamma = \gamma_- \cup \gamma_+$, *where* γ_- *and* γ_+ *denote the components below and above the singular line respectively, such that the closure* $\overline{\gamma}$ *intersects the singular line at a point which is not focal, is mapped by* T *in two disjoint unbounded arcs, doubly asymptotic to the line of focal values, with* $T(\gamma_-)$ *and* $T(\gamma_+)$ *below and above the line of focal values respectively.*

Remark 1. We may ask what happens when an arc γ is tangent to the singular line in a focal point, i.e. when $m = 0$. In this case the limit of $T(\gamma(t))$ goes to infinity, that is, the corresponding point $u_m(x^*) \to \pm\infty$ as $m \to 0$, the sign depending on the sign of $(f'(x^*) - 1)$ and on the arc γ. Thus for such an arc we have a behavior of $T(\gamma)$ similar to that occurring when γ intersects the singular line at a non focal point, that is, two disjoint unbounded arcs doubly asymptotic to the line of focal values.

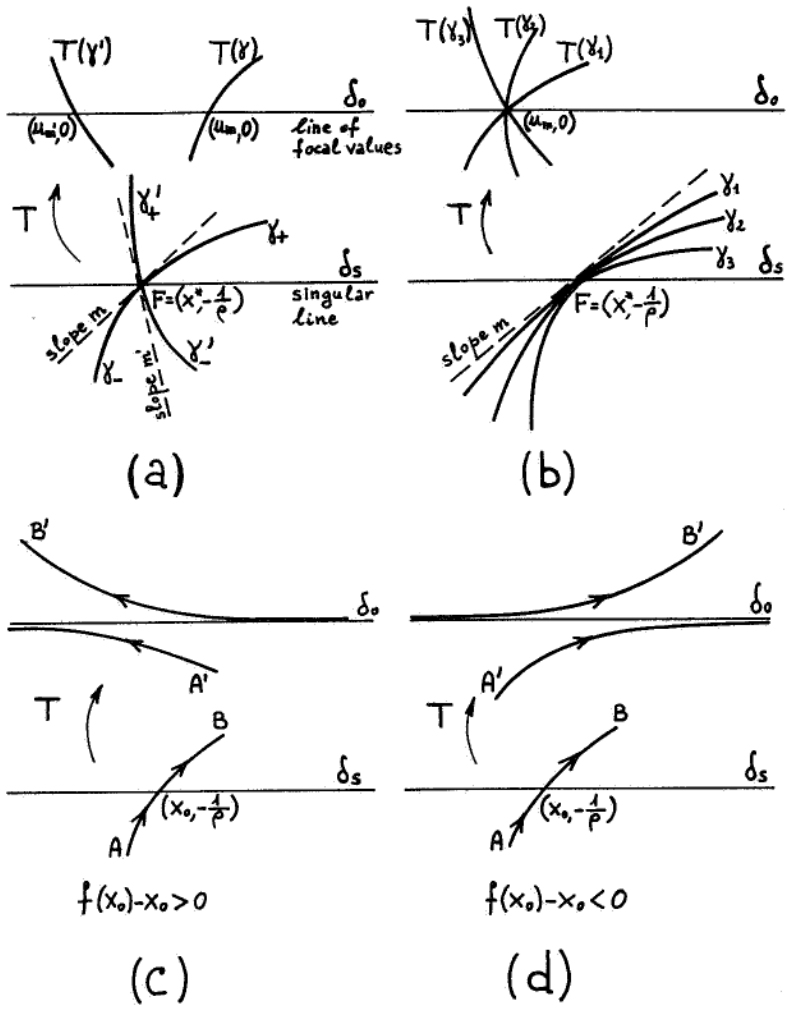

Fig. 1. (a) Smooth arcs crossing the singular line δ_s, through a focal point, with different slopes, are mapped by T into smooth arcs crossing the line of focal values δ_0 at distinct points whose coordinates are given by (15). (b) Smooth arcs crossing the singular line δ_s, through a focal point, with the same slope, are mapped by T into different arcs crossing the line of focal values δ_0 at the same point. (c) and (d) A smooth arc crossing the singular line δ_s, through a non focal point, is mapped by T into two disjoint unbounded arcs asymptotic to the line of focal values δ_0.

Proposition 2 suggests some consequences when we consider the preimages. The endomorphism in (1) may be a map with a non unique inverse, and the number of distinct inverses of T depends on the function $f(x)$, which is assumed to satisfy Assumption (H). In fact from Proposition 2 we can deduce that if $f(x)$ has N fixed points (hence also T has N fixed points) then the line of focal values must belong to a region, say Z_N, whose points have N distinct rank-1 preimages, as stated in the following:

Proposition 4. *Let $f(x)$ satisfy Assumption (H). If $f(x)$ has N fixed points then the line of focal values belongs to a region Z_N where T has N distinct inverses.*

In fact, under the assumptions of this proposition T has N disjoint focal points. If we consider disjoint neighborhoods U_i of the N focal points F_i, $i = 1, \ldots, N$ (deprived of the points of the singular line) then, for each i, $W_i = T(U_i)$ is a neighborhood of the line of focal values $y = 0$. The region $W = \bigcap_{i=1}^{N} W_i \neq \emptyset$ is an infinite strip containing the line of focal values. Let us denote by T_i^{-1} the inverse of T associated with the focal point F_i, that is, the inverse of T such that $T_i^{-1}(W) \subset U_i$. Then T has N distinct inverses defined in W, and each of them is associated with a focal point F_i, $i = 1, \ldots, N$.

From Proposition 2 we can also deduce the behavior of the rank-1 preimages of a smooth arc which intersects the line of focal values, say $\eta = \eta_- \cup \eta_+$, where η_- and η_+ denote the components

below and above the line of focal values respectively, and such that the closure $\overline{\eta}$ is smooth at the point $(u, 0)$ of intersection with that line. From Proposition 4 we can take the arc η entirely belonging to the region Z_N. Then the N distinct rank-1 preimages of η, say $T_i^{-1}(\eta)$, $i = 1, \ldots, N$, are arcs such that each closure $\overline{T_i^{-1}(\eta)}$ intersects the singular line at the focal point $F_i = (x_i^*, -\frac{1}{\rho})$, with slope m_i given by the relation $m_i(u) = \frac{f'(x_i^*)-1}{\rho(u-x_i^*)}$ obtained from (15) (see Fig. 2(a), where $N = 2$ is assumed). Note that the slope $m_i(u)$ is independent of the slope of the arc η and only depends on the focal point F_i and on the coordinate u at which $\overline{\eta}$ intersects the line of focal values. If we consider different arcs

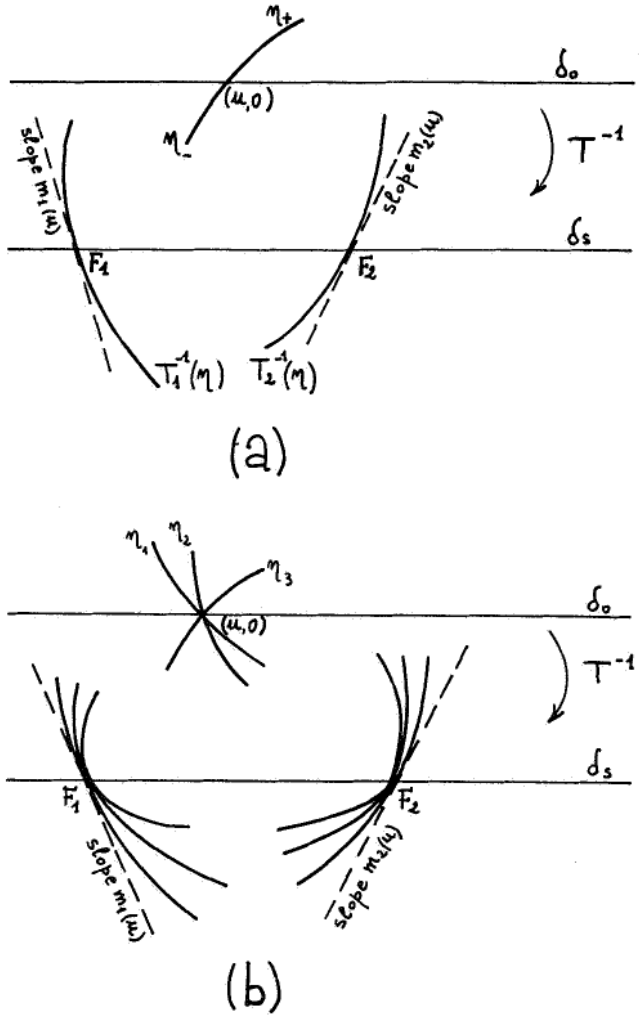

Fig. 2. (a) The rank-1 preimages of a smooth arc crossing the line of focal values δ_0 are arcs which "cross" the singular line δ_s through a focal point with slope given by (16). (b) The rank-1 preimages of smooth arcs crossing the line of focal values δ_0 at the same point $(u, 0)$ with different slopes m_i are given by arcs "crossing" the singular line δ_s at each focal point F_i with a slope only depending on u and F_i.

$\eta_\alpha = \eta_{\alpha-} \cup \eta_{\alpha+}$ belonging to region Z_N and such that all the closures $\overline{\eta_\alpha}$ are smooth and intersect the line of focal values at the same point $(u, 0)$ but with different slopes, then the rank-1 preimages of η_α, say $T_i^{-1}(\eta_\alpha)$, $i = 1, \ldots, N$, are such that all the arcs $\overline{T_i^{-1}(\eta_\alpha)}$, on varying α, intersect the singular line at the focal point F_i with the same tangent of slope $m_i(u)$ [see the qualitative picture in Fig. 2(b)]. In fact, assuming that one arc $\overline{T_i^{-1}(\eta_\alpha)}$ has a different slope, say p, then by applying the map T to it we get an arc crossing the line of focal values at the point $(u(p), 0)$, different from the starting point $(u, 0)$, which is a contradiction. Thus Proposition 2 admits a specular proposition which can be stated as follows:

Proposition 5. *Any smooth arc $\eta = \eta_- \cup \eta_+$, where η_- and η_+ denote the components below and above the line of focal values respectively, such that the closure $\overline{\eta}$ is smooth at the point $(u, 0)$ of intersection with that line, has preimage(s) $T_i^{-1}(\eta)$, $i = 1, \ldots, N$, such that each closure $\overline{T_i^{-1}(\eta)}$ intersects the singular line at the focal point $F_i = (x_i^*, -\frac{1}{\rho})$ with slope*

$$m_i(u) = \frac{f'(x_i^*) - 1}{\rho(u - x_i^*)}. \tag{16}$$

From Propositions 2 and 5 the following correspondence is obtained

Correspondence (slopes $\longleftrightarrow$ focal values) *The map T defines a one-to-one correspondence between the slopes of the lines $y = -\frac{1}{\rho} + m(x - x_i^*)$, $m \neq 0$, issuing from a focal point $F_i = (x_i^*, -\frac{1}{\rho})$, and the points $(u, 0)$ on the line of focal values, given by*

$$\begin{aligned} m \to (u, 0): &\quad u = x_i^* + \frac{f'(x_i^*) - 1}{\rho m} \\ (u, 0) \to m: &\quad m = \frac{f'(x_i^*) - 1}{\rho(u - x_i^*)}. \end{aligned} \tag{17}$$

Some consequences of the Correspondence (slopes $\longleftrightarrow$ focal values), important for the characterization of the basin boundaries and their bifurcations, are deduced by considering a smooth arc η such that $\overline{\eta}$ intersects the line of focal values at two points, say $(u, 0)$ and $(v, 0)$, as shown in Fig. 3(a). In this case η can be considered to be made up of three pieces, i.e. $\eta = \eta_1 \cup \eta_+ \cup \eta_2$, where η_1 and η_2 are below the line of focal values and η_+ is above it. As before, we can consider the arc η entirely

belonging to the region Z_N. Then, regardless of the values of u and v, the N rank-1 preimages of η, say $T_i^{-1}(\eta)$, $i = 1, \ldots, N$, are arcs such that each $\overline{T_i^{-1}(\eta)}$ has a loop in the focal point $F_i = (x_i^*, -\frac{1}{\rho})$ (see Fig. 3(a), where it is assumed $N = 2$). And also, as the slopes $m_i(u)$ and $m_i(v)$ are independent of the slope of the tangent to the starting arc $\overline{\eta}$ at the points $(u, 0)$ and $(v, 0)$, we can consider different arcs η_α such that all the closures $\overline{\eta_\alpha}$ are smooth and intersect the line of focal values in the same points $(u, 0)$ and $(v, 0)$ but with different slopes, and entirely belonging to the region Z_N. Then the rank-1 preimages of η_α, say $T_i^{-1}(\eta_\alpha)$, for $i = 1, \ldots, N$, and for any α, are such that the arcs $\overline{T_i^{-1}(\eta_\alpha)}$ form loops in the focal points, all having the same tangents in each F_i with slopes $m_i(u)$ and $m_i(v)$ according to (16) [see Fig. 3(b)]. Thus we have the following:

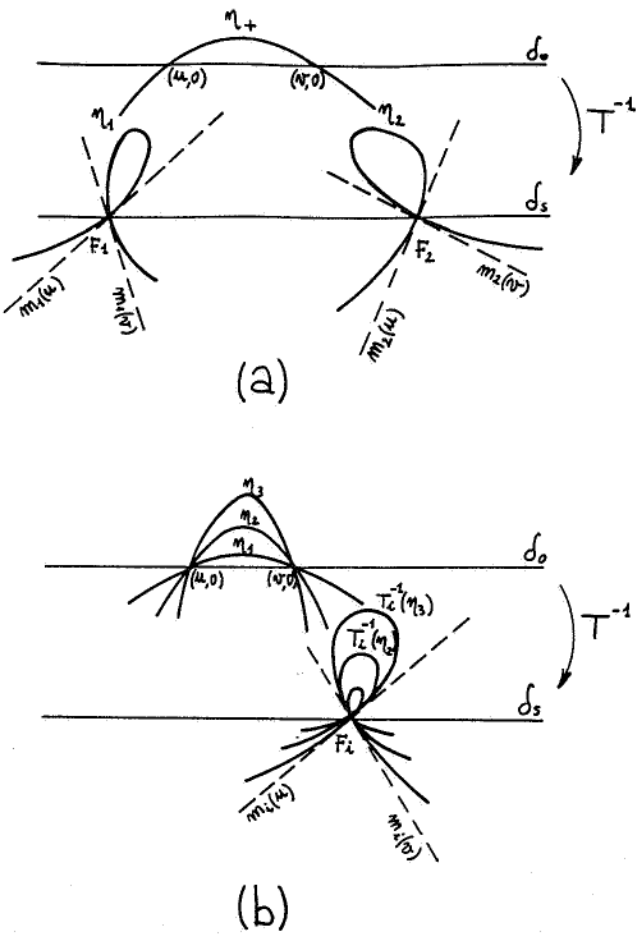

Fig. 3. (a) The preimage(s) of an arc crossing the line of focal values δ_s at two distinct points is (are) given by loop(s) issuing from the focal point(s). (b) The rank-1 preimages of a family of arcs crossing the line of focal values δ_0 at the same two distinct points are given by N families of nested loops issuing from the focal points, where N is the number of focal points.

Proposition 6. *Let $\eta = \eta_1 \cup \eta_+ \cup \eta_2$ be an arc, with components η_1 and η_2 below the line of focal values and η_+ above it, such that the closure $\overline{\eta}$ is smooth at the points $(u, 0)$ and $(v, 0)$ where it crosses the line of focal values. Let T_i^{-1} be an inverse of T which applies to all the points of η. Then the preimage $T_i^{-1}(\eta)$ is such that its closure $\overline{T_i^{-1}(\eta)}$ intersects the singular line at a focal point $F_i = (x_i^*, -\frac{1}{\rho})$ forming a loop with double point in F_i. The slopes of the two tangents in F_i are given by $m_i(u)$ and $m_i(v)$ according to (16).*

We close this section with some remarks.

Remark 2. We are tempted to include the focal points in the domain of T. In this case the new map, say $\overline{T}$, is single-valued in the set A and set-valued at the focal points, since $\overline{T}(F_i) = \delta_0$, where δ_0 denotes the line of focal values, for any F_i. Consequently, the range of $\overline{T}$ includes also the set of focal values, and each inverse $\overline{T}_i^{-1}$ of $\overline{T}$ is infinite-to-one in the line of focal values, being $\overline{T}_i^{-1}(\delta_0) = F_i$, $i = 1, \ldots, N$ (assuming that N focal points exist). However this extension is not satisfactory. In fact, if we consider a ball B as that shown in Fig. 4, deprived of its intersection with the line of focal values, then for any inverse T_i^{-1} we have that $T_i^{-1}(B)$ is an eight-shaped region, deprived of the focal point, and the points of B are in one-to-one correspondence with those of $T_i^{-1}(B)$. This correspondence is no longer preserved if we consider $\overline{T}$.

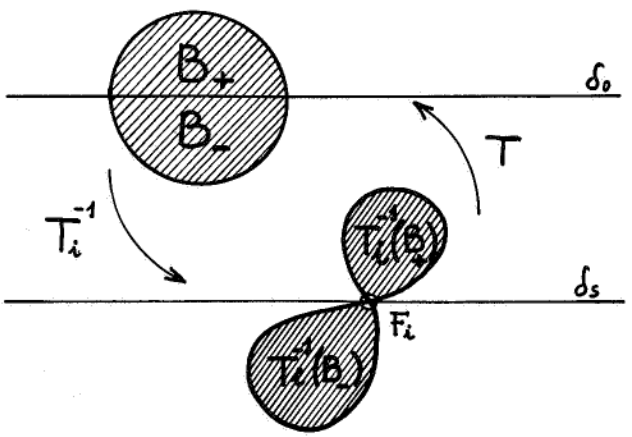

Fig. 4. Each preimage of a ball B, located partly above and partly below the line of focal values δ_0, is an eight-shaped region since the segment of δ_0 inside B is "focalized" into each focal point F_i by the inverse T_i^{-1}.

A good choice should be that of considering each focal point as an infinitesimal circle, and assigning the appropriate set of values to F_i (a subset of δ_0) obtained by the Correspondence (slopes $\longleftrightarrow$ focal values). This is just what T does.

Remark 3. The properties of the focal points F_i and of the set of the focal values δ_0 for the class of maps (1), given in Propositions 2–3 and 5–6, can be extended, with few changes, to a generic rational map with a vanishing denominator.

Remark 4. Even if for the class of maps studied in this paper we have that all the points at which a component assumes the form $\frac{0}{0}$ are focal points, for a generic rational map this may not be true. In fact a point at which a component of a rational map assumes the form $\frac{0}{0}$ but the limits of $T(\gamma(t))$ are divergent along any curve γ through it, does not behave as a focal point, but like any other point of the singular set (in which only the denominator vanishes). An example is the map considered in [Billings & Curry, 1996], where two points exist in which a component of the map becomes $\frac{0}{0}$, but only one is a focal point.

Remark 5. Consider a fold bifurcation of $f(x)$ which creates a pair of new fixed points of $f(x)$. Such a bifurcation creates a new pair of focal points for the triangular map T. At the bifurcation a fixed point ξ^* of $f(x)$ exists at which $f'(\xi^*) = 1$. In such a situation the set of focal values associated with the point $F = (\xi^*, -\frac{1}{\rho})$ is formed by the only point $(\xi^*, 0)$, according to (13). Thus the point F does not behave as a focal point, but we can considered it as a "germ" of true focal points since it splits into two focal points, whose set of focal values is the whole line $y = 0$, just after the bifurcation.

2.4. *Fan of stable sets issuing from the focal points and fractalization mechanism*

Although the line of focal values δ_0, of equation $y = 0$, does not belong to the range of T, it belongs to its domain A, and from (5) the image of rank-n of such line belongs to the line δ_n of equation $y = Y_n$ where

$$Y_n = \frac{1 - \rho^n}{1 - \rho} \tag{18}$$

i.e. the sequence $\{\delta_n\}$ is formed by lines parallel to the line of focal values δ_0 and convergent to the line of the ω-limit sets $y = y^*$, that can be denoted by δ_∞:

$$T^n(\delta_0) \subseteq \delta_n, \quad \text{with} \quad \delta_n \to \delta_\infty \quad \text{as} \quad n \to \infty. \tag{19}$$

From this observation follows that the stable set of any saddle cycle of T, obtained by taking the preimages of a local stable set, is made up of branches issuing from the focal points. In fact, the preimages of any local stable set, transverse to the line of ω-limit sets δ_∞, necessarily go back to the line of focal values δ_0 in a finite number of steps. Thus any stable set must be made of branches which "cross" the singular line at the focal points (for short, when we say that a branch "crosses" a point of the singular line, and in particular a focal point, it is implicitly understood that the point of the singular line is to be excluded). This means that, generally, a fan of branches of stable sets issues from any focal point, as we shall see in the example of Sec. 3 (see also [Bischi & Gardini, 1995]).

Proposition 7. *All the branches of stable sets of all the saddle cycles of T are "focalized" through the focal points of the maps (1).*

From (2) we know that all the preimages of a line δ_n belong to the line δ_{n-1}, $n \geq 1$. In particular $T_i^{-1}(\delta_1) = \delta_0$ for any inverse of T defined on the line δ_1 of equation $y = 1$. If we consider a smooth arc η crossing the line δ_1 at a point $(u_1, 1)$ we have that the arc $T_i^{-1}(\eta)$ intersects the line of focal values δ_0 at a point $(u_0, 0)$ and $T_{ii}^{-2}(\eta)$ "crosses" the singular line at a focal point F_i [see the qualitative picture in Fig. 5(a)]. The Fig. 5(b), where the situation of an arc η intersecting the line δ_1 at two points is considered, is self-explaining. If we consider an arc η which intersects both the lines δ_1 and δ_0 at two points, like in the Figs. 5(c) and 5(d), then $T_i^{-1}(\eta)$ "crosses" the singular line at a focal point F_i forming a loop which in turn intersects the line δ_0 at two points, say p_0 and q_0. Thus $T_{ii}^{-2}(\eta)$ "crosses" again the singular line at the focal point F_i with another loop whose slope depends on p_0 and q_0. We may have the second loop included in the previous one, as in Fig. 5(c), or out of it, as in Fig. 5(d). Taking into account the fact that the line of focal values belongs to a region Z_N, if the arc η entirely belongs to Z_N then $T^{-1}(\eta)$ includes $T_i^{-1}(\eta)$, $i = 1, \ldots, N$, that is N disjoint lobes (as in Fig. 5(e), where $N = 2$ is considered). If also these loops are all inside Z_N then each of them possesses N lobes as

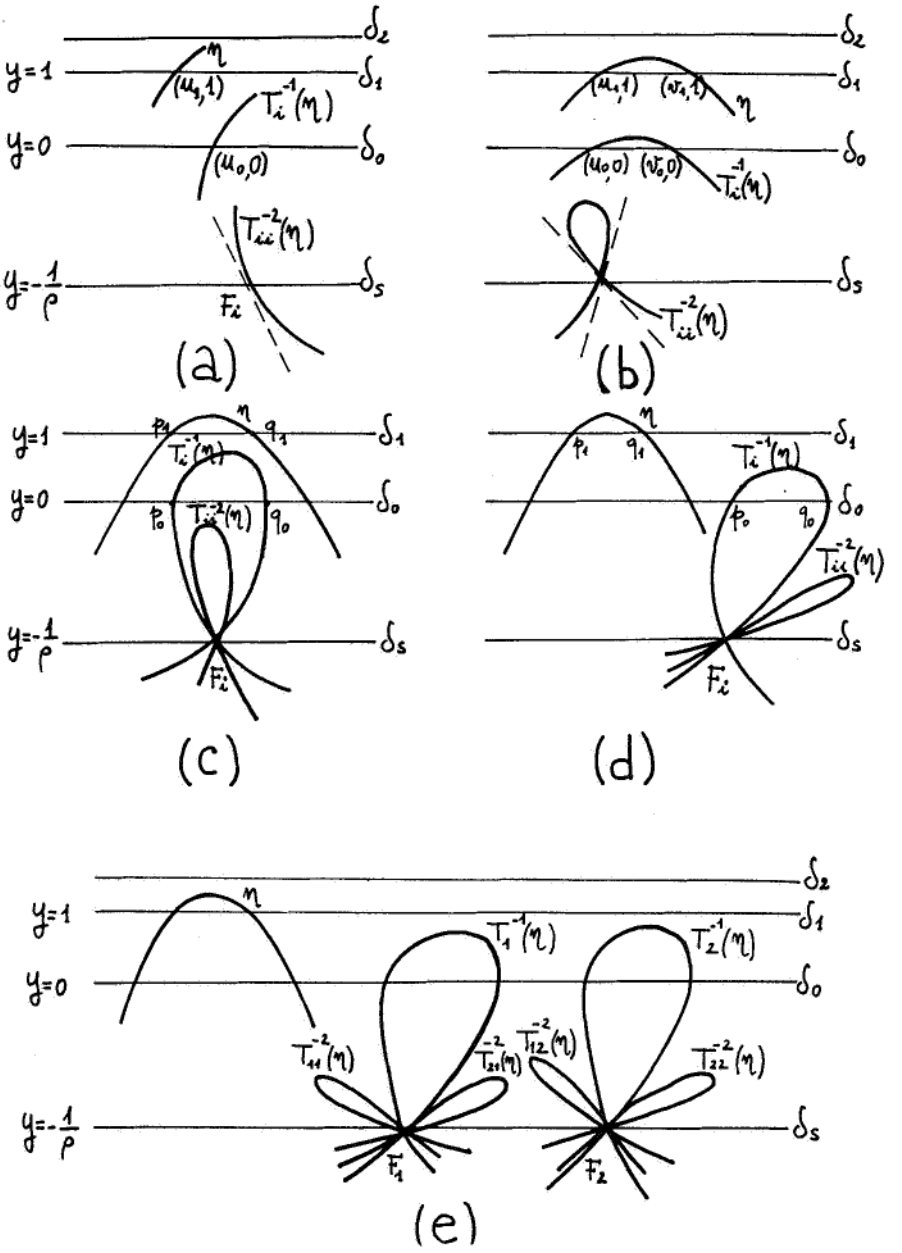

Fig. 5. The preimages of any arc crossing any line δ_n, and in particular those of the local stable sets of any saddle cycle located on δ_∞, are "focalized" in the focal points after a finite number of steps.

preimages, so that the rank-2 preimages $T_{i_1 i_2}^{-2}(\eta)$, where i_1 and i_2 take any value in $\{1, \ldots, N\}$, includes N^2 lobes.

It is clear now that if we consider an arc η which intersects the lines δ_j, $j = 0, 1, \ldots, (n-1)$ at two points, then the set of rank-n preimages $T^{-n}(\eta)$ includes at most N^n lobes issuing from the focal points $F_1, \ldots, F_N$.

This behavior, applied to the stable set of some saddle cycle, is at the basis of the fractalization of a basin boundary, as it will be shown in the example of Sec. 3.

2.5. *Critical curves LC_{-1} and LC of maps T*

From (8) the Jacobian of T is

$$J(x, y) = \det(DT(x, y)) = \rho \frac{\rho y + f'(x)}{1 + \rho y}. \quad (20)$$

It is immediate to see that any map (1) is *good* in Whitney's sense (see [Whitney, 1955]), that is at any point (x, y) of the domain A it is either $J(x, y) \neq 0$ or $J(x, y) = 0$ with $\text{grad}(J(x, y)) \neq 0$. In fact $\text{grad}(J(x, y)) = \rho[\rho \frac{f''(x)}{1+\rho y}, \frac{\rho(1-f'(x))}{(1+\rho y)^2}]$ has the

second component always different from zero when $J(x, y) \neq 0$. For a *good* map *the set* $J(x, y) = 0$ *consists of smooth curves* in A ([Whitney, 1955]). If T has more that one inverse then the set defined by the equation $J(x, y) = 0$ includes the critical curve of rank-0, denoted by LC_{-1} (see [Mira *et al.*, 1996]). It may happen that $LC_{-1} \subset \{(x, y) \mid J(x, y) = 0\}$, but for maps (1) LC_{-1} is exactly such set, i.e.

$$LC_{-1} = \left\{ (x, y) \,\middle|\, \frac{\rho y + f'(x)}{1 + \rho y} = 0, \quad y \neq -\frac{1}{\rho} \right\}. \tag{21}$$

In fact $J(x, y)$ cannot be factorized further, and it takes opposite signs on the two sides of the curve of the equation

$$y = -\frac{1}{\rho} f'(x) \tag{22}$$

which is the closure of LC_{-1}, say $\overline{LC_{-1}}$. For any point $(x, y) \in LC_{-1}$ we have $f'(x) \neq 1$, i.e.

$$(x, y) \in LC_{-1} \Longleftrightarrow y = -\frac{1}{\rho} f'(x) \quad \text{and} \quad f'(x) \neq 1 .$$

We note that while in maps defined in the whole plane the critical curve LC_{-1} separates regions where the Jacobian takes constant sign, in rational maps this may not be true. The class of maps (1) is an example: In fact in the region where $y > -\frac{1}{\rho} f'(x)$ we have $J(x, y) > 0$ (<0) for points above (below) the singular line $y = -\frac{1}{\rho}$.

A point $(x, y) \in LC_{-1}$ is mapped by T into a critical value, or critical point of rank-1

$$T\left(x, -\frac{1}{\rho} f'(x)\right) = \left(\frac{f(x) - x f'(x)}{1 - f'(x)}\, 1 - f'(x)\right) \quad \text{for any } x \text{ such that } \quad f'(x) \neq 1 . \tag{23}$$

If $\overline{LC_{-1}}$ intersects the singular line, necessarily at a point which is not focal if Assumption (H) holds, from Proposition 3 we have that LC includes disjoint branches doubly asymptotic to the line of focal values.

The vector tangent to LC_{-1} in (x, y) has the direction

$$\tau(x, y) = [\tau_1, \tau_2] = \frac{\rho}{1 + \rho y} [-\rho, f''(x)] \tag{24}$$

and the eigenvectors V_0 and V_ρ of $DT(x, y)$ which, when $(x, y) \in LC_{-1}$, correspond to the eigenvalues $s_1 = 0$ and $s_2 = \rho$, are given by

$$V_0(x, y) = [1, 0] \tag{25}$$

and

$$V_\rho(x, y) = \left[\frac{x - f(x)}{(1 - f'(x))^2}, 1\right]. \tag{26}$$

Thus when $f''(x) \neq 0$ the tangent to LC_{-1} at its point (x, y) is not parallel to the eigenvector $V_0(x, y)$. This is a sufficient condition for (x, y) to be a fold-point of LC_{-1}. Its image is a fold-point of LC, with tangent at the point $T(x, y)$ given by $V_\rho(x, y)$. This means that any smooth arc γ_α with tangent at (x, y) which is not parallel to $V_0(x, y)$ is mapped by T into a smooth arc tangent to LC at $T(x, y)$, i.e. "folded" on LC, and thus with tangent at $T(x, y)$ parallel to $V_\rho(x, y)$.

At a point $(x_s, y_s) \in LC_{-1}$ such that $f''(x_s) = 0$, the tangent to LC_{-1} is parallel to the eigenvector $V_0(x_s, y_s)$. Thus the point (x_s, y_s) may be a cusp-point of LC_{-1} and its image by T a cusp point of LC, according to Whitney [1955]. By applying Whitney's second order condition we get

$$\tau_1 \frac{\partial}{\partial x}(DT\tau) + \tau_2 \frac{\partial}{\partial y}(DT\tau) = -\frac{\rho^4}{(1 - f'(x_s))^2} f'''(x_s) V_\rho(x_s, y_s) .$$

Thus if $f'''(x_s) \neq 0$ the point (x_s, y_s) is a cusp-point. The slope of the tangent to the cusp of LC is given by the slope of $V_\rho(x_s, y_s)$.

These properties of the critical curves of T are summarized in the following:

Proposition 8. *Let $f(x)$ be a nonlinear function satisfying Assumption (H). Then*

(i) *The critical curve LC_{-1} has equation $y = -\frac{1}{\rho} f'(x)$, $y \neq -\frac{1}{\rho}$;*
(ii) *For any point $(x, y) \in LC_{-1}$ $f'(x) \neq 1$ holds;*
(iii) *If ξ exists such that $f'(\xi) = 1$ then $\overline{LC_{-1}}$ intersects the singular line in the non-focal point $(\xi, -\frac{1}{\rho})$;*
(iv) *If $\overline{LC_{-1}}$ intersects the singular line then LC has branches doubly asymptotic to the line of focal values;*
(v) *If $f''(x) \neq 0$ then the point $T(x, -\frac{1}{\rho} f'(x)) \in LC$ is a fold-point;*
(vi) *If $f''(x) = 0$ and $f'''(x) \neq 0$ then the point $T(x, -\frac{1}{\rho} f'(x)) \in LC$ is a cusp-point;*

(vii) *The tangent vector to a fold-point or a cusp-point* $T(x, -\frac{1}{\rho}f'(x)) \in LC$ *has slope* $\frac{(1-f'(x))^2}{x-f(x)}$.

2.6. *A peculiar role of the line of focal values*

That the preimages of points near the line of focal values are "focalized" at the focal points can also be seen directly by computing the rank-1 preimages (x, y) of a given point (x', y') in the range of T, i.e. with $y' \neq 0$. From the second component of T we get

$$y(x', y') = \frac{y' - 1}{\rho} \tag{27}$$

and $x(x', y')$ is a solution of the implicit equation

$$f(x) + (y' - 1)x - x'y' = 0\,. \tag{28}$$

As $y' \to 0$, $y(x', y') \to -\frac{1}{\rho}$ and $x(x', y') \to x_i^*$, where x_i^* is a fixed point of $f(x)$. In other words, if $y' \to 0$, $T_i^{-1}(x', y') = (x(x', y'), y(x', y'))$ tends to the focal point $F_i = (x_i^*, -\frac{1}{\rho})$, $i = 1, \ldots, N$, being N the number of fixed points of $f(x)$ which satisfies Assumption (H).

The property of *mapping arcs with different slopes into arcs with the same slope* is peculiar of the critical set LC_{-1}. As we have seen in Sec. 2.3 this behavior occurs for the inverses of T defined in a neighborhood of the line of focal values. This property of the line of focal values (perhaps unexpected) is stated in the following proposition:

Proposition 9. *Let* $f(x)$ *satisfy Assumption* (H). *For each of the inverses* T_i^{-1} *of* T *the Jacobian* $\det(DT^{-1}(x', y')) \to 0$ *as* (x', y') *tends to the line of focal values.*

In fact

$$\det(DT_i^{-1}(x', y')) = \frac{1}{\det(DT(x(x', y'), y(x', y'))}\,,$$

and from (20) we have

$$\det(DT_i^{-1}(x', y')) = \frac{y'}{\rho(y' + f'(x(x', y') - 1)} \to 0$$

as $y' \to 0$ because $x(x', y') \to x_i^*$ as $y' \to 0$, where x_i^* is a fixed point of $f(x)$, so that the denominator tends to $\rho(f'(x_i^*) - 1) \neq 0$ if Assumption (H) holds.

From Proposition 8, if we consider the eigenvalues σ_1 and σ_2 of $DT_i^{-1}(x', y')$, where $\sigma_1 \to 0$ as $y' \to 0$, with associated eigenvectors W_0 and W_ρ respectively, and apply T_i^{-1} to arcs "crossing" the line of focal values at a point $(x', 0)$, we obtain arcs "crossing" the focal points F_i with the same tangent, with slope equal to the slope of W_ρ as $y' \to 0$. Let us verify that the value $m_i(y')$ given in (16) is obtained following this procedure.

From the matrix DT given in (8) and from (28) we get

$$DT^{-1}(x', y') = \begin{bmatrix} \sigma_1 & \dfrac{x' - x(x', y')}{y' + f'(x(x', y')) - 1} \\ 0 & \sigma_2 \end{bmatrix}$$

with eigenvalues $\sigma_1 = \frac{y'}{y' + f'(x(x', y')) - 1}$ and $\sigma_2 = \frac{1}{\rho}$. The respective eigenvectors are

$$W_0(x', y') = [1, 0]$$

and

$$W_\rho(x', y') = \left[\frac{\rho(x' - x(x', y')}{y' + f'(x(x', y')) - 1}, 1\right].$$

As $y' \to 0$, considering the inverse T_i^{-1}, the eigenvector $W_\rho(x', y') \to [\frac{\rho(x' - x_i^*)}{f'(x_i^*) - 1}, 1]$ whose slope is $\frac{f'(x_i^*) - 1}{\rho(x' - x_i^*)}$, that is the value $m_i(x')$ expressed by (16), as expected.

3. A Particular Map T with Three Focal Points

In this Section we consider a particular map (1), obtained with a cubic function $f(x)$, defined by

$$f_\mu(x) = \mu x(1 - x)^2 \tag{29}$$

so that T becomes

$$T_{\rho\mu} : \begin{cases} x' = \dfrac{\rho xy + \mu x(1 - x)^2}{1 + \rho y} \\ y' = 1 + \rho y\,. \end{cases} \tag{30}$$

For $\mu > 0$ the function (29) satisfies Assumption (H) at the three fixed points

$$x_1^* = 0, \quad x_2^* = 1 - \frac{\sqrt{\mu}}{\mu}, \quad x_3^* = 1 + \frac{\sqrt{\mu}}{\mu}\,. \tag{31}$$

From Proposition 1 the map (30) has three focal points

$$F_k = \left(x_k^*, -\frac{1}{\rho}\right); \quad k = 1, 2, 3 \tag{32}$$

with x_k^* given by (31). The limiting function (7), which governs the asymptotic behavior of T, is given by the cubic map

$$h_{\rho\mu}(x) = x(\mu(1-\rho)x^2 - 2\mu(1-\rho)x + \mu(1-\rho) + \rho). \tag{33}$$

From the study of the derivative of (33) it is immediate to see that if

$$\mu > \frac{3\rho}{1-\rho} \tag{34}$$

then (33) is a bimodal map, with critical points

$$c_{-1} = \frac{1}{3}\left(2 - \sqrt{1 - \frac{3\rho}{\mu(1-\rho)}}\right) \text{ (local maximum)}$$

and

$$c'_{-1} = \frac{1}{3}\left(2 + \sqrt{1 - \frac{3\rho}{\mu(1-\rho)}}\right) \text{ (local minimum)} \tag{35}$$

otherwise it is an increasing map. As stated in Sec. 2.2, this map has the same fixed points (31) as the function $f_\mu(x)$, and from the study of $h'_{\rho\mu}(x)$ it is easy to see that x_3^* is a repelling fixed point for each $\mu > 0$, $\rho \in (0, 1)$. Also x_1^* is repelling for $\mu > 1$ (following this section, we shall only consider $\mu > 1$) whereas x_2^* is an attracting fixed point provided that

$$1 < \mu < \left(1 + \frac{1}{1-\rho}\right)^2. \tag{36}$$

At $\mu = (1 + \frac{1}{1-\rho})^2$ a flip bifurcation occurs at which x_2^* becomes repelling and a stable cycle of period two is created. If μ is further increased the period doubling route to chaos occurs, which creates cycles of each period 2^k, $k \in \mathbb{N}$, and then aperiodic (i.e. chaotic) bounded attractors. As it is well known, a bimodal map can have two coexisting bounded attractors (see e.g. [May, 1983; Mira, 1987; Milnor & Thurston, 1988; Uhl & Fournier–Prunaret, 1995]). That this also occurs for the map (33) can be seen from the bifurcation diagrams of Fig. 6, obtained with a fixed value of the parameter ρ and by varying the bifurcation parameter μ. The upper bifurcation diagram shown in Fig. 6 is obtained by taking the critical point c_{-1} as the initial condition for each value of μ, whereas the lower one is obtained with the initial condition always taken at the other critical point, c'_{-1}. From a comparison of the two bifurcation diagrams it is evident that two simultaneous attractors coexist for μ values taken in a given range. For example, with $\rho = 0.18$ and $\mu = 8.93$ an attracting cycle of period 2 coexists with an attracting cycle of period 4, as it is shown in the two Koenig–Lemeray staircase diagrams of Fig. 6. Moreover, for $\mu > 1$, positively (negatively) unbounded dynamics of the limiting map (33) are obtained with initial conditions $x > x_3^*$ ($x < x_1^*$). However unbounded dynamics can also be obtained starting with initial conditions taken from subsets of the interval (x_1^*, x_3^*) whenever the relative maximum value $c = h_{\rho\mu}(c_{-1})$ is greater than x_3^*. The creation of such "holes" occurs when $h_{\rho\mu}(c_{-1}) = x_3^*$ as in Fig. 7(a), where the "germs" of the holes, given by the critical point c_{-1} and its preimages, are indicated. In Fig. 7(b), obtained with a greater value of μ, the holes inside (x_1^*, x_3^*), whose points generate unbounded sequences, are evidenced by the thicker portions on the diagonal, and a typical divergent trajectory, starting from one of the holes, is shown. In this case any bounded sequence generated by $h_{\rho\mu}(x)$ enters the absorbing interval (c', c'_1) where $c' = h_{\rho\mu}(c'_{-1})$ is the local minimum value and $c'_1 = h_{\rho\mu}(c')$, but when μ reaches the value at which $c'_1 = h_{\rho\mu}(x_3^*)$ a *final bifurcation* occurs at which the absorbing interval is destroyed, and the generic trajectory of the map (33) is divergent. This condition represents, for the limiting map (33), the contact of the absorbing interval (c', c'_1), with the basin of infinity [Fig. 7(c)].

As stressed in Sec. 2.2, a complete knowledge of the properties of the limiting map is necessary in order to understand the asymptotic dynamics of the triangular map T. The map $T_{\rho\mu}$ defined in (30) has three fixed points, located on the line of the ω-limit sets $y = y^*$, given by

$$Q_k = (x_k^*, y^*), \quad k = 1, 2, 3$$

with x_k^* given by (31) and y^* given by (6). For $\mu > 1$ both Q_1 and Q_3 are saddle points with unstable manifold along the invariant line $y = y^*$ and local stable set on the lines perpendicular to it, i.e. $x = x_1^*$ and $x = x_3^*$ respectively. The fixed point Q_2 is an attracting node as long as (36) holds and becomes

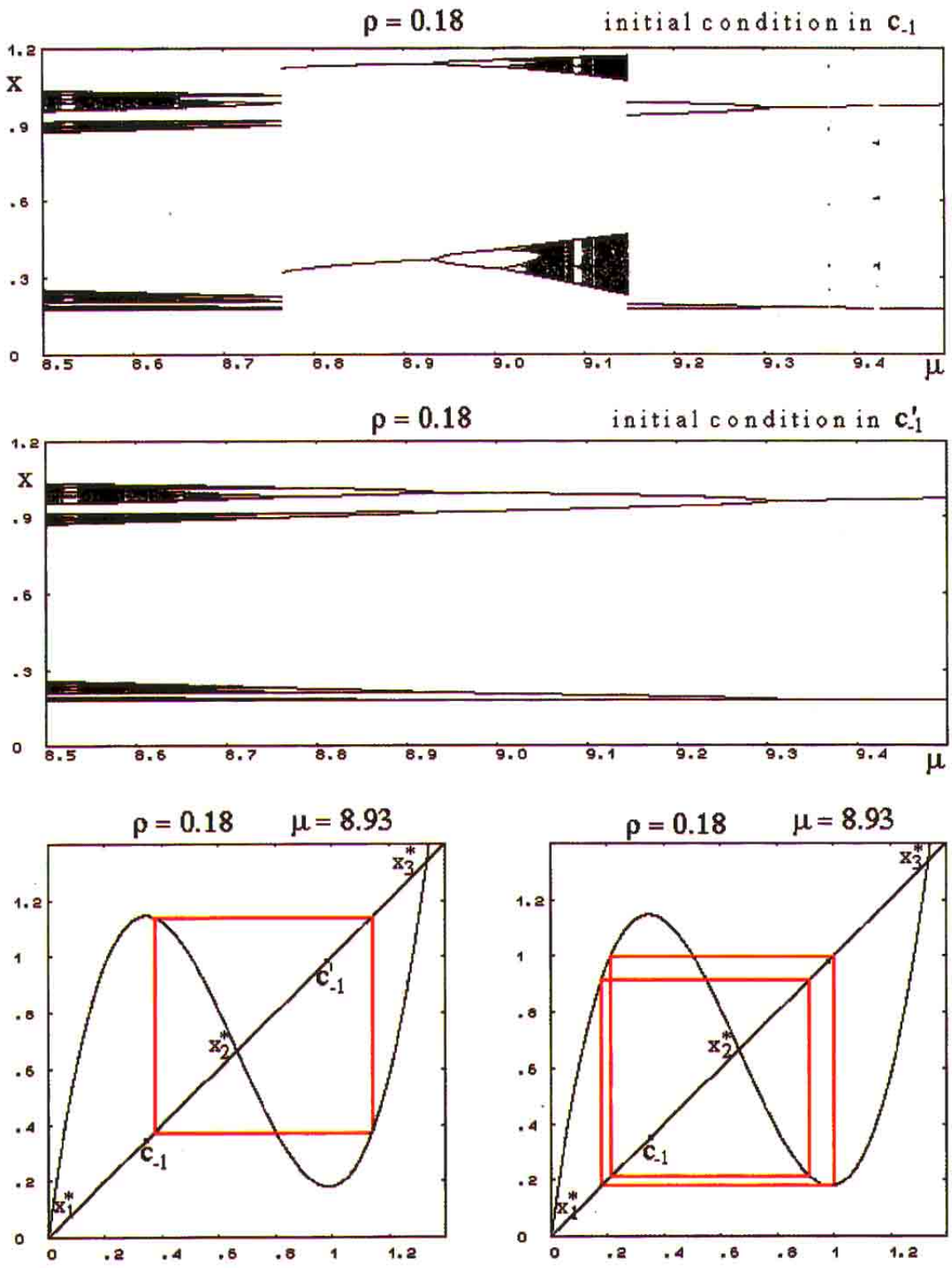

Fig. 6. Coexisting bounded attractors of the bimodal limiting map $h_\rho(x)$ can be evidenced by comparing the two bifurcation diagrams obtained with the initial condition taken in the relative maximum point c_{-1} and the relative minimum point c'_{-1} respectively. With the value $\mu = 8.93$ of the bifurcation parameter an attracting cycle of period 2 coexists with an attracting cycle of period 4, as shown in the two Koenig–Lemeray staircase diagrams.

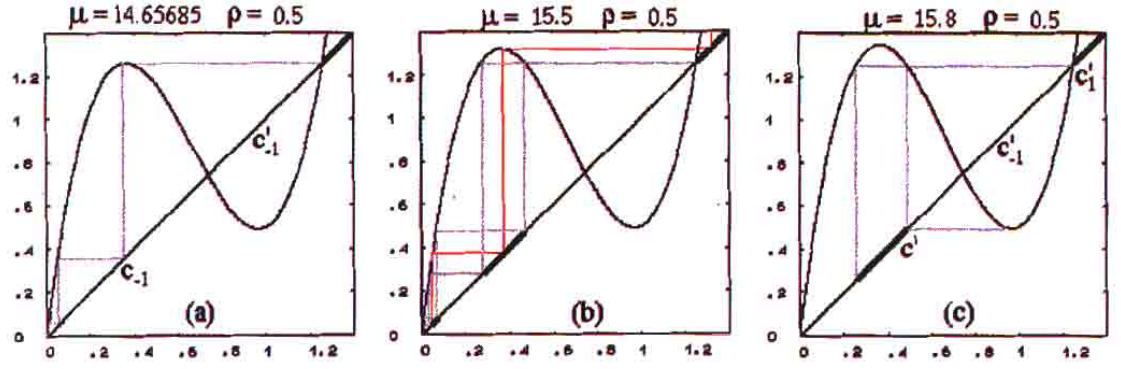

Fig. 7. Three situations which characterize the behavior of the limiting map $h_\rho(x)$. The thicker portions of the diagonal represent sets of points which generate unbounded trajectories of $h_\rho(x)$. In (a) the condition $c' = h_\rho(c'_{-1}) = x_3^*$ hold, hence the critical point c'_{-1} and its infinite preimages represent "germs" of holes, inside the interval (x_1^*, x_3^*), whose points generate unbounded trajectories of $h_\rho(x)$. In (b), obtained with a larger value of μ, some of these holes are shown together with a typical diverging trajectory starting from one of these holes. In (c) the condition $c'_1 = h_\rho(c') \equiv x_3^*$ holds. This represents the "final bifurcation" at which any bounded attractor of the limiting map (and hence also of the triangular map T) is destroyed.

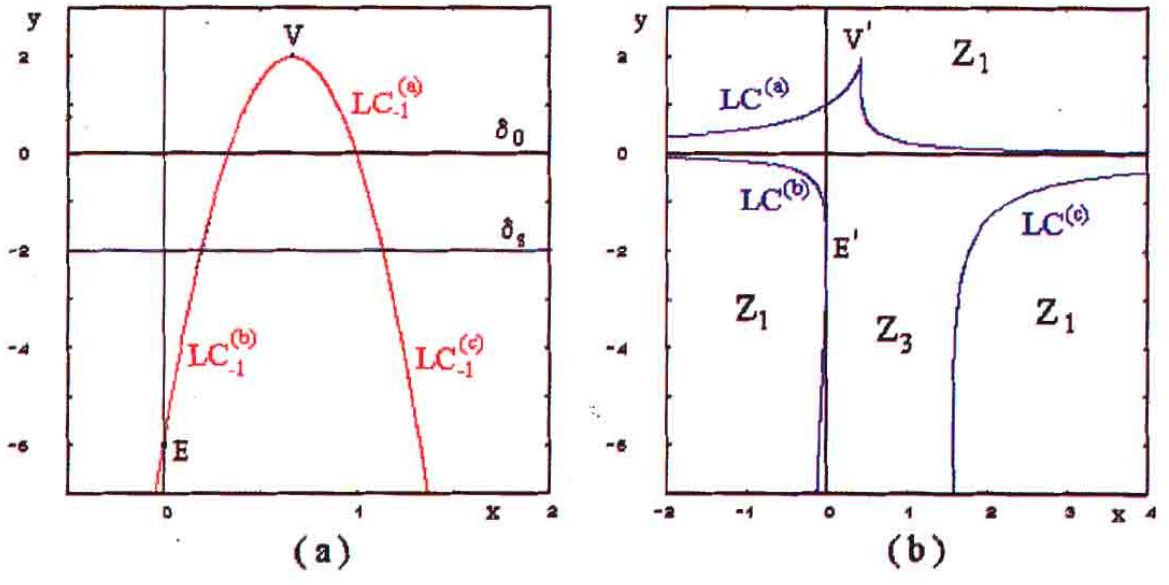

Fig. 8. In (a) the three branches of the critical curve of rank-0 LC_{-1}, located on a parabola and separated by the singular line δ_s, are shown. In (b) the corresponding three branches of the critical curve of rank-1 LC are shown.

a saddle point, with unstable set along the line $y = y^*$, after the flip bifurcation occurring at $\mu = (1 + \frac{1}{1-\rho})^2$, at which an attracting node cycle of period 2, say $\{(x_1, y^*), (x_2, y^*)\}$, appears, where $\{x_1, x_2\}$ is the stable 2-cycle of the limiting map (33). More generally, as stated in Sec. 2.2, every attractor of the limiting map (33) gives a corresponding attractor of the triangular map (30), located on the line $y = y^*$.

As stressed in Sec. 2, the delimitation of the basins of the different attractors of the map $T_{\rho\mu}$ requires a global study of the map (30), taking into account its critical sets and the particular properties related to the presence of focal points. The map (30) is a noninvertible map defined in the set A given in (4). Its Jacobian matrix has determinant $J(x, y)$ vanishing along the curve of the equation

$$y = -\frac{\mu}{\rho}(3x^2 - 4x + 1), \quad y \neq -\frac{1}{\rho}. \tag{37}$$

According to part (i) of Proposition 8 the curve LC_{-1} for the map (30) is formed by the three arcs of the parabola (37) separated by the singular line δ_s. In Fig. 8 these arcs are denoted by $LC_{-1}^{(a)}$, which

represents the portion of parabola above the singular line and containing the vertex $V = (\frac{2}{3}, \frac{\mu}{3\rho})$, which from Proposition 8 is the unique cusp-point (in Whitney's sense) of LC_{-1}, $LC_{-1}^{(b)}$, which is the infinite branch below the singular line intersecting the y-axis in the point $E = (0, -\frac{\mu}{\rho})$, and $LC_{-1}^{(c)}$, representing the other infinite branch below the singular line.

Also the curve LC of critical values, obtained as $LC = T(LC_{-1})$ with LC_{-1} given by (37), is formed by three branches, as shown in Fig. 8, given by $LC^{(a)} = T(LC_{-1}^{(a)})$, located above the line of the focal values $y = 0$ and containing the cusp-point $V' = T(V) = (\frac{8}{9}\frac{\mu}{\mu+3}, \frac{\mu+3}{3})$, $LC^{(b)} = T(LC_{-1}^{(b)})$, tangent to the y-axis at the point $E' = T(E)$ and $LC^{(c)} = T(LC_{-1}^{(c)})$, tangent to the line $x = x_3^*$ at the point $T(x_3^*, 1 - f'(x_3^*))$. According to Proposition 8 the line of focal values δ_0, of equation $y = 0$, is an asymptote for all the three branches, since the curve LC_{-1} "crosses" the singular line out of the focal points.

After some algebraic manipulations the following expression of LC is obtained:

$$x = \frac{2}{27y}\left[\mu + 9y - 9 \pm (\mu + 3 - 3y)\sqrt{\frac{\mu + 3 - 3y}{\mu}}\right] \qquad y \neq 0\,. \tag{38}$$

It can be noticed that LC intersects the line of ω-limit sets $y = y^*$ only when (34) is satisfied, and in this case the x coordinates of the two intersection points are the critical values of the limiting map, given by

$$\begin{aligned} &c = h_{\rho\mu}(c_{-1}) && \text{(maximum value)} \\ &\text{and} && (39) \\ &c' = h_{\rho\mu}(c'_{-1}) && \text{(minimum value)} \end{aligned}$$

where c_{-1} and c'_{-1} are given in (35).

According to Proposition 4 the line of focal values $y = 0$ belongs to a region Z_3, whose points have three distinct rank-1 preimages. This region extends to the whole zone between the branches $LC^{(b)}$ and $LC^{(c)}$ and below $LC^{(a)}$. The complementary zones of the range of T, separated from Z_3 by the branches of LC, are denoted as Z_1 regions, since their points have a unique rank-1 preimage. For any point (x', y') in the range of the map (30), i.e. with $y' \neq 0$, the coordinates (x, y) of the preimages (one or three) can be obtained as the solutions of the system of equations

$$\begin{cases} \mu x^3 - 2\mu x^2 + (\mu - 1 + y')x - x'y' = 0 \\ y = \dfrac{y' - 1}{\rho} \end{cases} \tag{40}$$

obtained from (28) and (27) respectively. As already stressed in Sec. 2, even if the line of focal values δ_0 does not belong to the range of T, we can consider such line as belonging to region Z_3, in the sense that points arbitrarily close to this line have three distinct preimages that are close to the three focal points (32).

By using (40) we can obtain the boundary ∂D_∞ which separates the basin D_∞, defined as the set of points which generate unbounded trajectories of the map (30), from the set of points generating bounded trajectories. As the boundary of D_∞ must include the saddle fixed points Q_1 and Q_3, and no other cycle of $T_{\rho\mu}$ exists out of the line $y = y^*$, the whole boundary ∂D_∞ is given by the stable sets of these two saddles, formed by the union of the preimages of their local stable sets, lying on the lines $x = x_1^*$ (say ω_1) and $x = x_3^*$ (say ω_3) respectively:

$$\partial D_\infty = W^s(Q_1) \cup W^s(Q_3)$$

where

$$W^s(Q_1) = \bigcup_{n\geq 0} T^{-n}(\omega_1)$$

and

$$W^s(Q_3) = \bigcup_{n\geq 0} T^{-n}(\omega_3)\,.$$

The set of rank-1 preimages of a point of ω_1, say $(0, y')$ with $y' \neq 0$, can easily be obtained from (40). In this case the cubic equation which implicitly defines the x coordinates of the preimages assumes the simpler form

$$x(\mu x^2 - 2\mu x + \mu - 1 + y') = 0 \tag{41}$$

which always admits the solution $x = 0$, corresponding to the preimage $T_1^{-1}(0, y') = (0, \frac{y'-1}{\rho})$ located on the same line ω_1 [this is consistent with the fact that every line $x = x_k^*$, with x_k^* given in (31), is an invariant line for the triangular map (30)]. Two further preimages

$$\begin{aligned} &T_2^{-1}(0, y') = \left(1 - \sqrt{\frac{1 - y'}{\mu}}, \frac{y' - 1}{\rho}\right) \\ &\text{and} && (42) \\ &T_3^{-1}(0, y') = \left(1 + \sqrt{\frac{1 - y'}{\mu}}, \frac{y' - 1}{\rho}\right) \end{aligned}$$

exist provided that $y' \leq 1$, that is, if the point $(0, y')$ belongs to Z_3, being $(0, 1)$ the intersection point of LC with the line ω_1. The two branches of preimages () form the set of rank-1 preimages of ω_1 out of itself, which will be denoted as ω_1^{-1}. Such a set is located on the parabola of the equation

$$y = -\frac{\mu}{\rho}(x-1)^2 \tag{43}$$

which represents the closure $\overline{\omega_1^{-1}}$, since ω_1^{-1} is deprived of the points on the singular line. The parabola (43) has vertex $(1, 0)$, at which the two branches () merge, belonging to the curve LC_{-1}, and crosses the singular line at the focal points F_2 and F_3, according to Proposition 7 (see Fig. 9). Preimages of a higher rank of the line ω_1, which can be obtained by applying T^{-1} to the points of ω_1^{-1}, are all in the half-plane below the singular line for each value of the parameters. This is due to the fact that the vertex of ω_1^{-1} always belongs to the line $y = 0$ independently of the parameters' values, so that ω_1^{-1} has no arcs above the line of focal values.

A more interesting situation is obtained when the preimages of the line ω_3, of equation $x = x_3^*$, are considered. Also in this case the analytical expression of the rank-1 preimages can be easily obtained. In fact the cubic equation in (40), with the coordinates of the generic point of ω_3, given by $(1+\frac{\sqrt{\mu}}{\mu}, y')$ with $y' \neq 0$, becomes

$$(x - x_3^*)(\mu x^2 + (\sqrt{\mu} - \mu)x + y') = 0\,.$$

Thus x_3^* is always a solution, i.e. $T_3^{-1}(x_3^*, y') = (x_3^*, \frac{y'-1}{\rho})$, being the line $x = x_3^*$ invariant for T, and other two preimages,

$$T_1^{-1}(x_3^*, y') = \left(\frac{\mu - \sqrt{\mu} - \sqrt{(\mu-\sqrt{\mu})^2 - 4\mu y'}}{2\mu}, \frac{y'-1}{\rho}\right)$$

and (44)

$$T_2^{-1}(x_3^*, y') = \left(\frac{\mu - \sqrt{\mu} + \sqrt{(\mu-\sqrt{\mu})^2 - 4\mu y'}}{2\mu}, \frac{y'-1}{\rho}\right)$$

exist provided that $y' \leq \frac{(\mu-\sqrt{\mu})^2}{4\mu}$, the right hand side of this inequality being the y coordinate of the intersection of LC with the line ω_3. Also in this case the set of preimages of the line ω_3 out of itself, say ω_3^{-1}, is located on a parabola, of equation

$$y = -\frac{1}{4\rho\mu}[-4\mu x^2 + 4\mu(\mu - \sqrt{\mu})x + \mu^2 - 2\mu\sqrt{\mu} - 2\sqrt{\mu} - 4\mu - 1]\,, \tag{45}$$

which crosses the singular line at the focal points F_1 and F_2, and has vertex

$$B = \left(\frac{1}{2}\left(1 - \frac{\sqrt{\mu}}{\mu}\right), \frac{\mu - 2\sqrt{\mu} - 3}{4\rho}\right) \tag{46}$$

on the curve LC_{-1} (Fig. 9).

Differently from ω_1^{-1} the vertex of the parabola ω_3^{-1} moves upwards as the parameter μ increases (or ρ decreases). As long as the vertex B is below the line of focal values δ_0 all the preimages of ω_3^{-1} are below the singular line δ_s, and lobes of D_∞ are not present [this is the situation shown in Fig. 9(a)]. If we increase the value of parameter μ the curve ω_3^{-1} becomes tangent to the line of focal values when the y coordinate of the vertex B vanishes, i.e. at $\mu = \mu_1^* = 9$. At this value of the parameter μ the first bifurcation of D_∞, due to a contact of ∂D_∞ with the line of focal values δ_0, occurs. In fact, for $\mu > \mu_1^*$ an arc of ω_3^{-1}, containing the vertex B, is above the line of focal values and intersects it at two points. In such a situation Proposition 6 implies that the three preimages $T_i^{-1}(\omega_3^{-1})$, $i = 1, 2, 3$, form loops issuing from the focal points F_i, $i = 1, 2, 3$, so that the effect of this basin bifurcation is given by the first creation of lobes of D_∞ [see Fig. 9(b)]. These three lobes belong to the set of preimages of rank-2 of the local stable set ω_3, and will be denoted as ω_3^{-2}.

If μ is further increased other bifurcations, at which new lobes of D_∞ issuing from the focal points are created, occur when old lobes reach the line of focal values. In fact when the vertex B of ω_3^{-1} reaches the line δ_1, of equation $y = 1$, its rank one preimages B_{-1}, which are on the top of the three lobes ω_3^{-2}, reach the line δ_0 of focal values. This gives the second basin bifurcation, occurring at $\mu = \mu_2^* = (1+2\sqrt{1+\rho})^2$, at which 3^2 new lobes are created, issuing from the focal points. These lobes, rank-1 preimages of the three lobes ω_3^{-2} whose upper parts are above the line of focal values δ_0 for $\mu > \mu_2^*$, will be denoted as ω_3^{-3} [see Fig. 10(a)].

Following the same arguments outlined at the end of Sec. 2.4, we can state that at any contact of ω_3^{-1} with a line of the sequence $\{\delta_n, n \geq 0\}$, where δ_n has equation $y = Y_n$ with Y_n given by (18), causes the creation of new lobes, say ω_3^{-n}, issuing

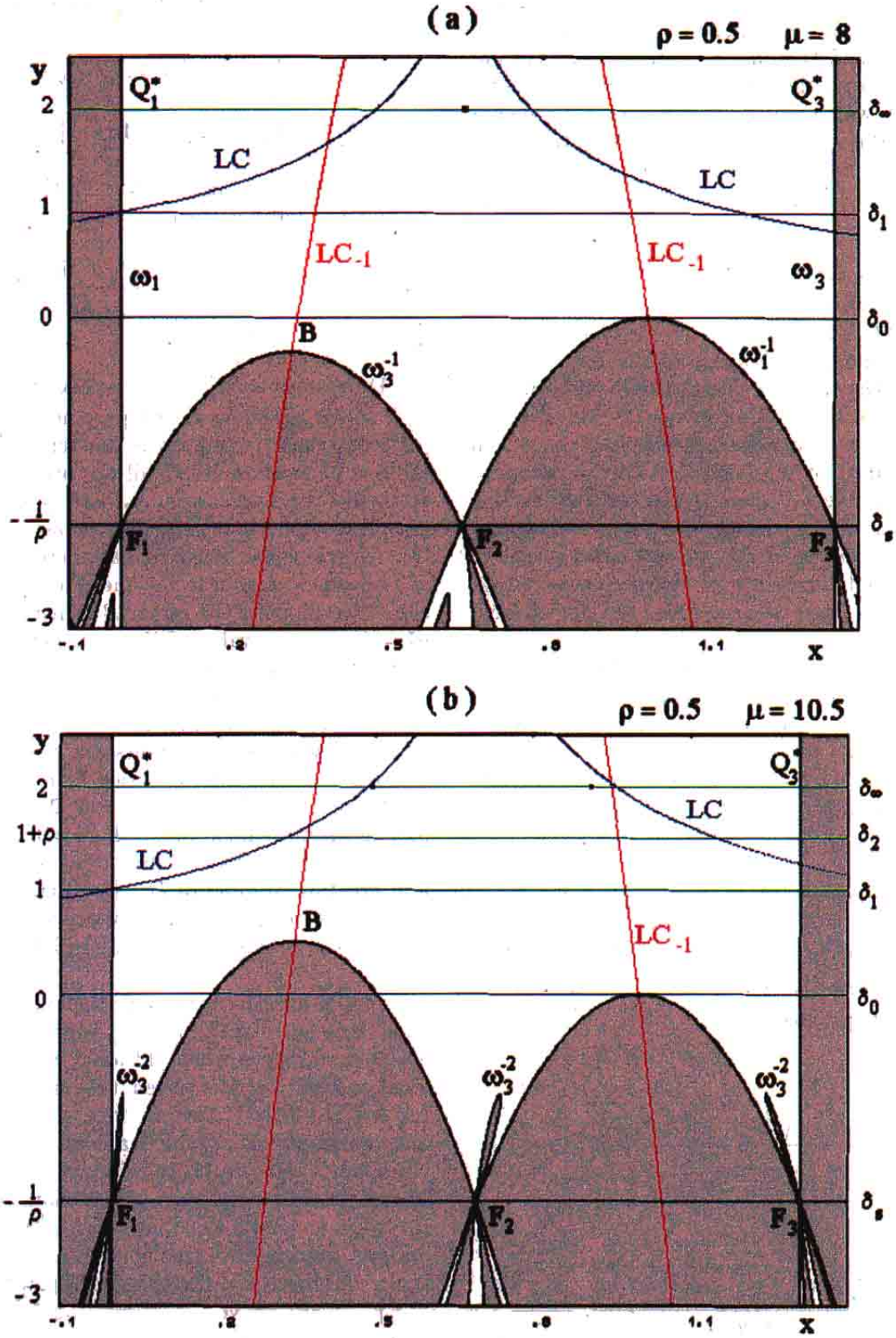

Fig. 9. The grey-shaded area represents the basin D_∞ of diverging trajectories of the map $T_{p\mu}$, the white region represents the basin of bounded trajectories. In both these figures all the bounded trajectories converge to the same attractor, namely the fixed point x_2^* in Fig. 9(a) and an attracting 2-cycle in Fig. 9(b), represented by the brown dots on the line δ_s of the ω-limit sets. The boundary ∂D_∞ which separates the two basins is given by the stable sets of the two saddles Q_1^* and Q_3^*, obtained as the union of the preimages of their local stable sets, denoted by ω_1 and ω_3 respectively. In (a) $\mu < \mu_1^*$ and in (b) $\mu_1^* < \mu < \mu_2^*$.

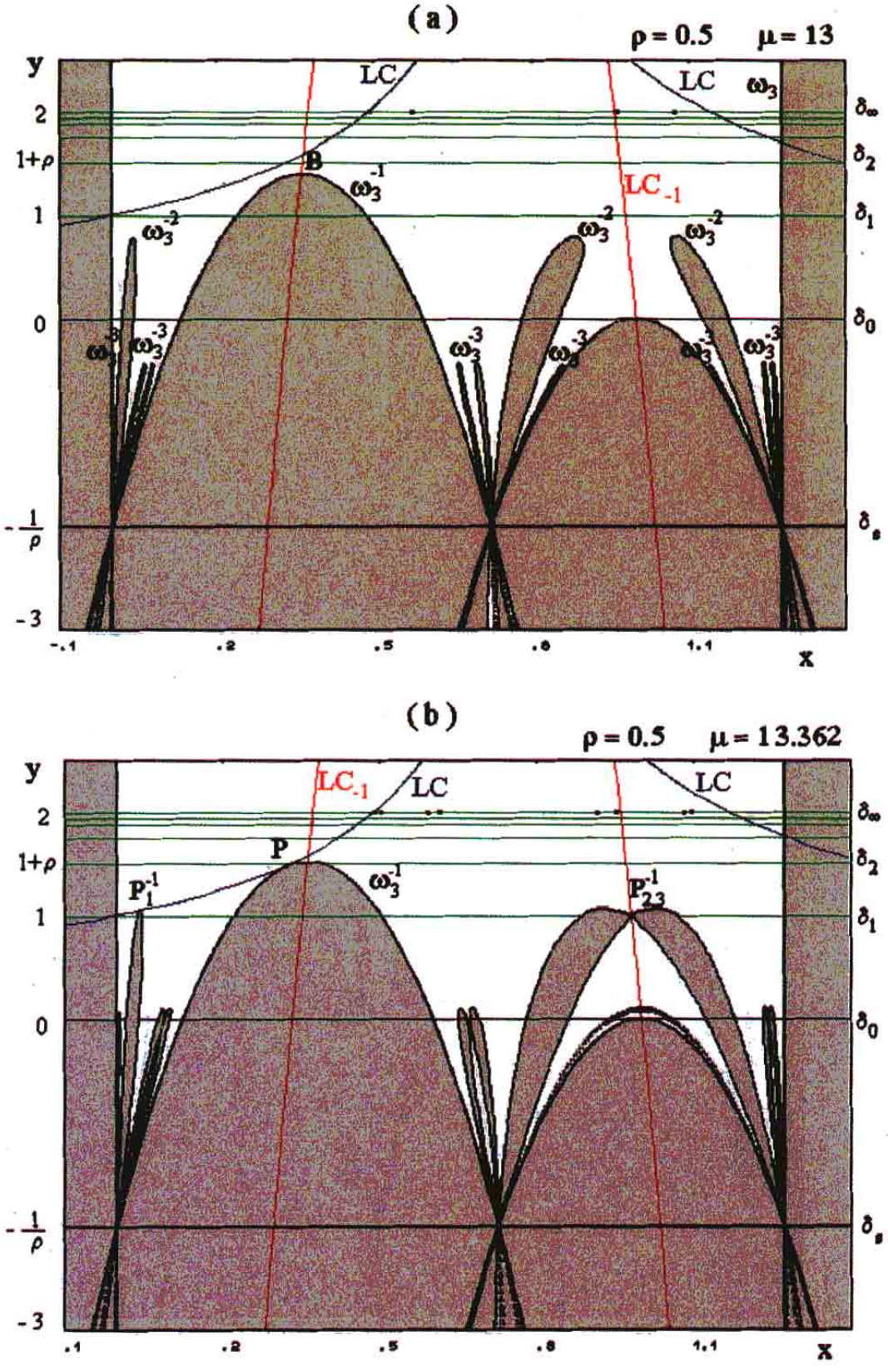

Fig. 10. (a) The vertex B of the parabola ω_3^{-1} is above the line δ_1 and below the line δ_2, i.e. $\mu_2^* < \mu < \mu_3^*$, so that the 3^2 new lobes created at the contact of the three lobes ω_3^{-2} with δ_0 can be seen, denoted by ω_3^{-3}. (b) The contact of ω_3^{-1} with LC causes the merging of lobes and the creation of "arcs", bounded half-moon shaped regions of basins issuing from the focal points.

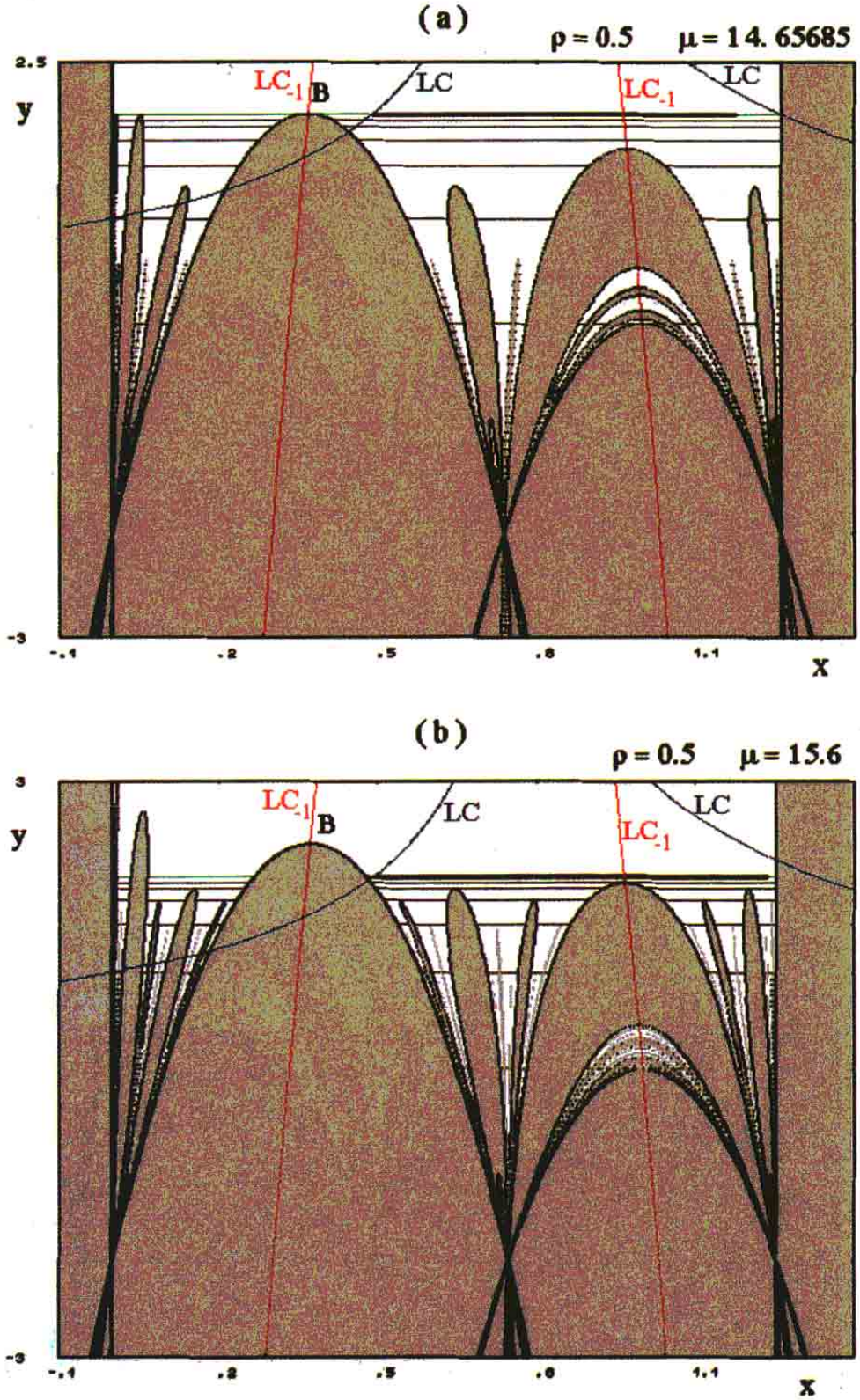

Fig. 11. (a) The vertex B of the parabola ω_3^{-1} is tangent to the line δ_∞ of ω-limit sets, and the tangency point belongs to region Z_1 where only one inverse exists. This implies that the infinite preimages $T_1^{-i}(\omega_3^{-1})$, $i = 1, \ldots, \infty$, are lobes all tangent to the same line (even if only two of them, on the left of ω_3^{-1}, are visible in the figure). (b) The vertex of the parabola ω_3^{-1} is now above the line δ_∞ and the same is true for all its preimages. The intersection of these infinite lobes, accumulating near the y-axis, and the line δ_∞, gives infinite holes of the limiting map $h_{\rho\mu}(x)$ as shown in Fig. 7(b).

from the focal points (32). Such contact occurs at the μ value at which the vertex B of ω_3^{-1} belongs to the line δ_n, i.e. when

$$\mu = \mu_n^* = (1 + 2\sqrt{1 + \rho Y_n})^2 \qquad (47)$$

with Y_n given in (18).

Besides the creation of new lobes, through the sequence of bifurcations described above, due to contacts between ∂D_∞ and the line of focal values, merging of lobes can occur as a consequence of contacts of ∂D_∞ and the critical curve LC. For example, in Fig. 10(b) the portion of ∂D_∞ formed by ω_3^{-1} is tangent to LC at the point P. The two preimages of P, $T_2^{-1}(P) \equiv T_3^{-1}(P)$, located on LC_{-1}, are the contact points of the two rightmost lobes ω_3^{-2}, and preimages of higher rank of P are contact points of all the lobes which are preimages of these [see Fig. 10(b)]. This basin bifurcation, due to a contact of ∂D_∞ with LC, is a known bifurcation, whose mechanism is described in detail in [Mira *et al.*, 1996] and in the previous works of the same authors, like [Mira *et al.*, 1994; Mira & Rauzy, 1995]. The merging of lobes causes the creation of disjoint regions of the basin of bounded trajectories surrounded by D_∞, which will be denoted by the term "arcs". This may be considered as a new mechanism of formation of basin structures similar to the "islands" described in [Mira *et al.*, 1994]. Note that, after the contact with LC, ω_3^{-1} enters the region Z_1, so further contacts of this curve with the lines δ_n occur at points of Z_1.

As μ is further increased the parabola ω_3^{-1} crosses other lines of the sequence $\{\delta_n\}$ until it reaches the line of the ω-limit sets δ_∞. The contact between ω_3^{-1} and the line of ω-limit sets occurs at $\mu = \mu_\infty^*$, where $\mu_\infty^* = \lim_{k\to\infty} \mu_k^* = (1 + 2\sqrt{\frac{1}{1-\rho}})^2$.

At this value of μ an infinite number of lobes has been created, preimages of ω_3^{-1}, and all these infinite lobes, located on the left of the isolated lobe given by $T_1^{-1}(\omega_3^{-1})$, are tangent to the line $y = y^*$ [Fig. 11(a)]. In Fig. 11(a) infinite preimages of the point B accumulate on the fixed point $Q_1^* = (0, y^*)$, although only two of such lobes can be seen. All these infinitely many lobes intersect LC, and their preimages have infinitely many "connections" on LC_{-1}, thus creating infinite "white" and "grey" half-moon shaped *arcs* between the focal points F_2 and F_3 [although only few of them are visible in Fig. 11(a)]. This bifurcation on the line of ω-limit sets can be well understood if we look at

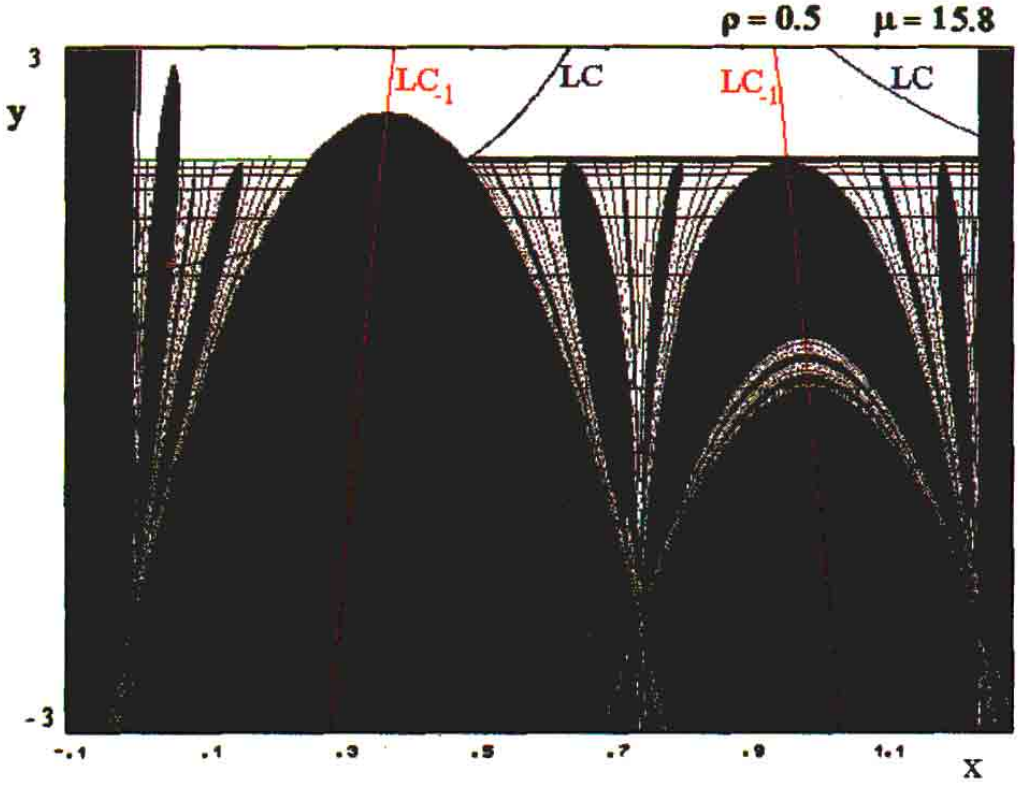

Fig. 12. A contact of ∂D_∞ with the line δ_s of the ω-limit sets occurs at a point of the region Z_3 where three distinct inverses exist. The contacts of ∂D_∞ with the infinite sequence of lines $\{\delta_n\}$ has created an exponentially increasing number of lobes issuing from the three focal points. At the contact the basin boundary assumes a fractal structure.

the restriction of T to this line, that is, the limiting map (33). In fact at $\mu = \mu^*_\infty$ the critical curve LC crosses the line of ω-limit sets in the saddle point $Q_3 = (x^*_3, y^*)$. This means that the local maximum value of the limiting map $c = h_{\rho\mu}(c_{-1})$ coincides with x^*_3, as in Fig. 7(a). The tangency point of ω_3^{-1} with δ_∞ is the critical point c_{-1} of the limiting map $h_{\rho\mu}(x)$, and the other infinite contact points of ∂D_∞ with the same line are given by the infinite preimages $c_{-n} = h^{-n}_{\rho\mu}(c_{-1})$, $n \in \mathbb{N}$, which accumulate at $x = 0$.

As μ is increased beyond μ^*_∞, as in Fig. 11(b), all these lobes cross the line of the ω-limit sets thus giving infinite holes on that line [compare Fig. 11(b) to Fig. 7(b)].

In the meantime, due to the increase of μ, also the lobes $T_2^{-1}(\omega_3^{-1})$ and $T_3^{-1}(\omega_3^{-1})$, that merged at the contact of ω_3^{-1} with LC, have moved upwards and, crossing more and more lines l^k_s, have created more and more new lobes. The merging of the two lobes gives an *arc* of D_∞, say $\mathcal{A}_1$, which at its creation only intersects the line δ_1, but as μ increases intersects all δ_n at points belonging to Z_3. This causes a sequence of bifurcations whose effect is a process of creation of lobes typical of the fractal figures. In fact, when $\mathcal{A}_1$ intersects δ_2 then 3^2 lobes intersect δ_0 and 3^3 lobes issue from the three focal points, and so on. All the lobes issuing from the focal points F_2 and F_3 always belong to region Z_3, hence, when $\mathcal{A}_1$ intersects δ_n at least 2^n lobes intersect δ_0 and 2^{n+1} new lobes issue from the focal points F_2 and F_3. As $n \to \infty$ we obtain a fractal basin because the lobes created by this process can be put in a one-to-one correspondence with the elements of the "middle-third" Cantor set. Also in this case the limiting value of μ, say μ_F, at which $\mathcal{A}_1$ has a contact with the line of ω-limit sets can be computed from the limiting map (33), since it corresponds to the situation shown in Fig. 7(c). Thus the value of μ_F can be deduced from the condition $c'_1 = h_{\rho\mu}(c') = x^*_3$, where c' represents the local minimum value of the limiting function. When $\mu = \mu_F$ infinite contacts of ∂D_∞ with the line δ_0 occur, since the infinite lines of the sequence δ_n have

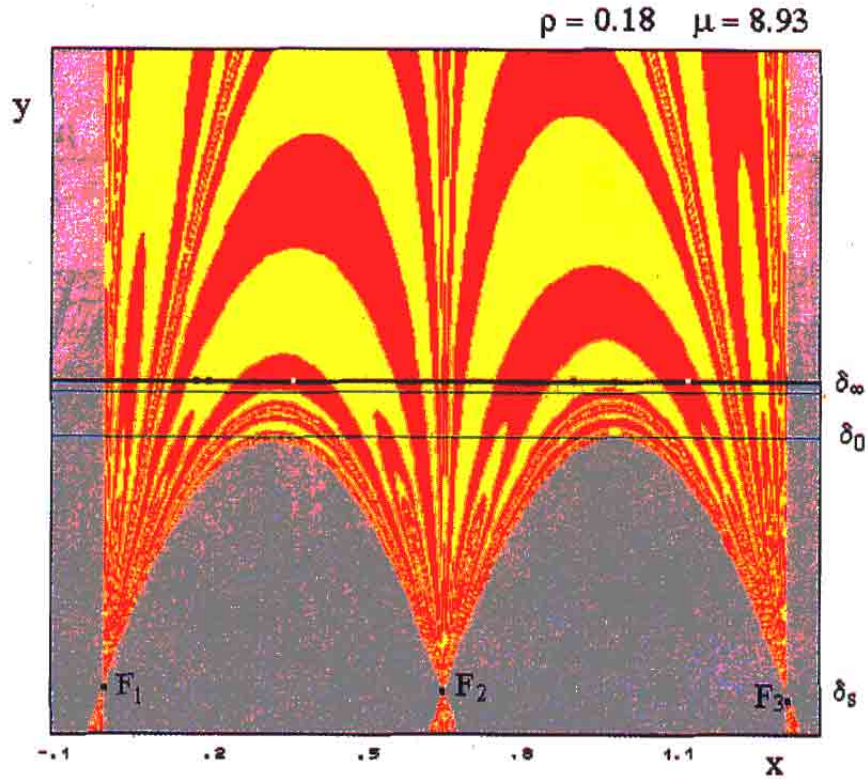

Fig. 13. This figure is obtained with the same values of the parameters ρ and μ as those used in Fig. 6, so that two simultaneous bounded attractors, namely an attracting 2-cycle and an attracting 4-cycle, coexist. In this case the basin of bounded trajectories can be further subdivided into the basins of the two attracting cycles. In this figure the red colored region represent the set of points whose trajectories converge to the 2-cycle, the yellow one represents the basin of the 4-cycle. The cycles are represented by small dots on the line δ_∞ of the ω-limit sets: The white dots represent the 2-cycle and the black ones represent the 4-cycle. The two basins are clearly characterized by structures of lobes and arcs issuing from the focal points.

been crossed, so that all the lobes have been created and have reached the limit line δ_∞ (see Fig. 12). Also for the map T this is the *final bifurcation* at which any bounded absorbing set is destroyed (see [Mira *et al.*, 1996] or [Abraham *et al.*, 1996]), and the generic trajectory of the triangular map (30) is divergent.

At this value of the parameter μ the boundary of D_∞ has assumed a typical fractal structure, and if μ is further increased infinite holes are created inside the interval (x_1^*, x_3^*) where the ω-limit set was located. Thus the bounded attractors are destroyed and only a repelling invariant Cantor set survives.

When more coexisting bounded attractors of the map T are present on the line of ω-limit sets, like in the case shown in Fig. 13, the set of points generating bounded trajectories, represented by the white areas in the Figs. 10–12, can be further subdivided into the basins of the different attractors. In Fig. 13, obtained with the same set of parameters as in Fig. 6, the basins of attraction of the stable node-cycles of period 2 and 4 are represented by different colors, red and yellow respectively, whereas the grey regions represent, as in the previous figures, the basin of infinity. This figure clearly shows that the boundary which separates the two basins of the bounded attractors is formed by fans of curves issuing from the three focal points. Such a boundary is formed by the stable sets of saddle-cycles located between the attracting node-cycles. As explained in Sec. 2, these stable sets, obtained as the union of all the preimages of the local stable of the saddle cycles which are always transverse to the line $y = y^*$, must necessarily cross the singular line through the focal points, thus giving basin structure with lobes and arcs.

Acknowledgments

The authors wish to thank an anonymous referee for interesting comments. They also thank Prof. C. Mira for very useful discussions on the topic of this paper.

The work has been performed under the activity of the national research project "*Dinamiche non lineari ed applicazioni alle scienze economiche e sociali*", MURST, Italy, and under the auspices of GNFM, CNR, Italy.

References

Abraham, R., Gardini, L. & Mira, C. [1997] *Chaos in Discrete Dynamical Systems* (*A Visual Introduction in Two Dimensions*), (Springer-Verlag, Berlin).

Billings, L. & Curry, J. H. [1996] "On noninvertible mappings of the plane: Eruption points," *Chaos* **6**(2), 108–120.

Bischi, G. I. & Gardini, L. [1995] "Mann iterations reducible to plane endomorphisms," *Quaderni di Economia, Matematica e Statistica* **36**, (Università di Urbino).

Bischi, G. I. & Gardini, L. [1996] "A class of nonautonomous processes solved via two-dimensional maps," submitted.

Bischi G. I. & Naimzada, A. [1995] "A cobweb model with learning effects," *Atti XIX Convegno AMASES* (Cacucci Editore, Bari), pp. 162–177.

Bischi, G. I. & Naimzada, A. [1996] "A dynamic duopoly game with local adaptive response," submitted.

Gardini, L. & Mira, C. [1993] "On the dynamics of triangular maps," *Dinamiche non lineari ed applicazioni alle scienze economiche e sociali* working paper No. 9305, Progetto Nazionale di Ricerca MURST.

Gumowski, I. & Mira, C. [1980] *Dynamique Chaotique* (Cepadues Editions, Toulose).

May, R. M. [1983] "Nonlinear problems in ecology and resource management," in *Chaotic Behavior of Deterministic Systems*, eds. Iooss, G., Helleman, R. G. H. & Stora, R. (North Holland Pub. Co.) pp. 516–563.

Milnor, J. & Thurston, W. [1988] "On iterated maps of the interval," in *Lecture Notes in Mathematics*, **1342**, ed. Alexander J. (Springer-Verlag, Berlin).

Mira, C. [1981] "Singularités non classiques d'une récurrence, et d'une équation differentielle d'ordre 2," *Comptes Rendus Acad. Sc. Paris, Série I* **292**, 147–151.

Mira, C. [1987] *Chaotic Dynamics* (World Scientific, Singapore).

Mira, C., Fournier–Prunaret, D., Gardini, L., Kawakami, H. & Cathala, J. C. [1994] "Basin bifurcations of two-dimensional noninvertible maps: Fractalization of basins," *Int. J. Bifurcation and Chaos* **4**, 343–381.

Mira, C., Gardini, L., Barugola, A. & Cathala, J. C. [1996] *Chaotic Dynamics in Two-Dimensional Noninvertible Maps* (World Scientific, Singapore).

Mira, C. & Rauzy, C. [1995] "Fractal Aggregation of Basin Islands in Two-Dimensional Quadratic Noninvertible Maps," *Int. J. Bifurcation and Chaos* **5**, 991–1019.

Uhl, C. & Fournier–Prunaret, D. [1995] "Chaotic phenomena in an order 1 DPCM transmission system," *Int. J. Bifurcation and Chaos* **5**, 1033–1070.

Whitney, H. [1955] "On singularities of mappings of euclidean spaces. I. Mappings of the plane into the plane," *Annals of Mathematics* **62**, 374–410.